

1 **Disease Resistance Genetics and Genomics in Octoploid Strawberry**

2 Christopher Barbey^{*,‡}, Seonghee Lee[†], Sujeet Verma[†], Kevin A. Bird^{§,**}, Alan E. Yocca^{††}, Patrick
3 P. Edger^{§,**}, Steve J. Knapp^{‡‡}, Vance M. Whitaker[†] and Kevin M. Folta^{*,‡}

4
5 ^{*} Horticultural Sciences Department, University of Florida, Gainesville FL USA

6 [†] Gulf Coast Research and Education Center, University of Florida, Wimauma, FL USA

7 [‡] Graduate Program in Plant Molecular and Cellular Biology, University of Florida, Gainesville,
8 FL USA

9 [§] Department of Horticulture, Michigan State University, East Lansing, MI, USA

10 ^{**} Ecology, Evolutionary Biology and Behavior, Michigan State University, East Lansing, MI,
11 USA

12 ^{††} Department of Plant Biology, Michigan State University, East Lansing, MI, USA

13 ^{‡‡} Department of Plant Sciences, University of California, Davis, Davis, CA, USA

14

15

16 Octoploid Strawberry R-genes
17 Strawberry, Disease Resistance, R-gene, eQTL, Subgenome Dominance, RenSeq
18 Dr. Christopher Barbey
19 Horticultural Sciences Department
20 University of Florida
21 Gainesville FL 32611
22 208-585-7967
23 cbarbey@ufl.edu
24

25 **ABSTRACT**

26 Octoploid strawberry (*Fragaria ×ananassa*) is a valuable specialty crop, but profitable production
27 and availability are threatened by many pathogens. Efforts to identify and introgress useful disease
28 resistance genes (R-genes) in breeding programs are complicated by strawberry's complex
29 octoploid genome. Recently-developed resources in strawberry, including a complete octoploid
30 reference genome and high-resolution octoploid genotyping, enable new analyses in strawberry
31 disease resistance genetics. This study characterizes the complete R-gene collection in the
32 genomes of commercial octoploid strawberry and two diploid ancestral relatives, and introduces
33 several new technological and data resources for strawberry disease resistance research. These
34 include octoploid R-gene transcription profiling, *dN/dS* analysis, eQTL analysis and RenSeq
35 analysis in cultivars. Octoploid fruit transcript expression quantitative trait loci (eQTL) were
36 identified for 77 putative R-genes. R-genes from the ancestral diploids *Fragaria vesca* and
37 *Fragaria iinumae* were compared, revealing differential inheritance and retention of various
38 octoploid R-gene subtypes. The mode and magnitude of natural selection of individual *F.*
39 *×ananassa* R-genes was also determined via *dN/dS* analysis. R-gene sequencing using enriched
40 libraries (RenSeq) has been used recently for R-gene discovery in many crops, however this
41 technique somewhat relies upon *a priori* knowledge of desired sequences. An octoploid strawberry
42 capture-probe panel, derived from the results of this study, is validated in a RenSeq experiment
43 and is presented for community use. These results give unprecedented insight into crop disease
44 resistance genetics, and represent an advance towards exploiting variation for strawberry cultivar
45 improvement.

46

47 **INTRODUCTION**

48 Cultivated strawberry (*Fragaria ×ananassa*) is an important specialty crop that is cultivated
49 world-wide for its sweet and flavorful fruit. However, marketable yields and post-harvest quality
50 are significantly affected by disease. The strawberry fruit presents a vulnerable target for microbial
51 pathogens (Farzaneh *et al.*, 2015), as it is soft, moist, carbohydrate rich, and subject to damage
52 from forces as seemingly innocuous as rain (Herrington *et al.*, 2011). Genetic disease resistance
53 has been a long-standing breeding priority. While breeders have made progress in producing
54 varieties with tolerance to some pathogens, growers remain dependent on exogenous crop
55 protection strategies to reduce pathogen loads (Cordova *et al.*, 2017).

56 Plant R-genes are mediators of resistance to specific pathogens via effector triggered immunity,
57 which results in the hypersensitive response and cell death (Amil-Ruiz *et al.*, 2018). R-genes
58 require a high degree of regulation to maintain homeostatic transcript levels to mitigate off-target
59 protein interactions (Hammond-Kosack and Jones, 1997). For this reason, many classes of
60 functional R-genes are expressed at low levels unless elicited by pathogens (Lai and Eulgem,
61 2017), contributing to the challenges of R-gene genomic and functional annotation. About 60% of
62 characterized plant R-genes contain nucleotide-binding (NB-ARC) and leucine-rich-repeat (LRR)
63 domains, and are referred to NLR genes (Funk *et al.*, 2018). Plant R-genes are frequent targets for
64 genetic improvement via breeding and genetic engineering (Djian-Caporalino *et al.*, 2014,
65 Baumgartner *et al.*, 2015), and gene editing methods may accelerate their introduction into
66 already-elite varieties. However, progress has been hindered because relatively few R-genes
67 conferring novel resistance have been characterized (Amil-Ruiz *et al.*, 2018). This problem is
68 appreciable in strawberry, where the genetic complexity of octoploid cultivars presents unique
69 challenges for functional identification and cloning of causal variants. An analysis of diploid R-
70 genes across the Rosaceae genus was previously conducted (Arya *et al.*, 2014). New genetic
71 resources for high-resolution genotyping in octoploid strawberry have resulted in the recent
72 identification of several disease resistance loci (Roach *et al.*, 2016, Mangandi *et al.*, 2017, Anciro
73 *et al.*, 2018, Pincot *et al.*, 2018, Salinas *et al.*, 2018, Verma *et al.*, 2018). However, the specific
74 genes mediating resistance in these QTL intervals typically remain unresolved, as genomic
75 resources for octoploid strawberry have not kept pace with genetic mapping.

76 Cultivated strawberry shares common ancestors with the extant diploid species *F. vesca*, *F.*
77 *iinumae*, *F. nipponica*, and *F. viridis* (Edger *et al.*, 2019). A high-quality octoploid strawberry

78 genome has been recently developed (Edger *et al.*, 2019), enabling new kinds analyses and
79 improved resolution compared with previous studies involving *Fragaria* NLRs (Jia *et al.*, 2015,
80 Zhong *et al.*, 2018). Analysis of this *F. ×ananassa* ‘Camarosa’ genome identified the repertoire
81 of octoploid R-gene sequences and further demonstrated a general genomic retention bias towards
82 *F. vesca*-like sequences (Edger *et al.*, 2019).

83 This research compares R-genes from octoploid strawberry with its diploid ancestors and provides
84 additional analysis into the genetic control of R-gene expression and retention patterns. Additional
85 bias towards retention of *F. vesca*-like R-genes was detected in octoploid strawberry, beyond the
86 bias observed in non-R-gene coding sequences. This finding provides insight into potential
87 practical drivers of biased gene retention. Conserved domains were compared to describe specific
88 R-gene phylogenic relationships. The octoploid genome was used to assemble 61 fruit
89 transcriptomes, and used to discover subgenomic expression quantitative trait loci (eQTL) for R-
90 genes expressed in octoploid fruit. Data from the octoploid ‘Camarosa’ strawberry gene expression
91 atlas (Sánchez-Sevilla *et al.*, 2017) was also used to determine R-gene transcript accumulation
92 throughout the strawberry plant.

93 Resistance gene enrichment and sequencing (RenSeq) is an advantageous method for sequencing
94 R-genes (Andolfo *et al.*, 2014), and is likely to be very useful for *de novo* resolution of causal
95 mutations (Witek *et al.*, 2016). This method can be used to identify casual mutations within
96 existing disease resistance QTL. For this purpose, a novel octoploid strawberry RenSeq capture
97 probe library was designed using the R-genes identified in this analysis. This panel was
98 experimentally validated using the University of Florida breeding germplasm. The results
99 demonstrate robust capture and resequencing of octoploid and diploid R-genes using only short
100 second-generation sequence reads and with relatively deep genomic multiplexing.

101 This report characterizes the complete R-gene collection in the genomes of commercial octoploid
102 strawberry and two diploid ancestral relatives, providing the genome-level resolution necessary
103 for fully exploiting genetic disease resistance in strawberry. This research introduces several new
104 technology and data resources that now may be applied in study of strawberry disease resistance.

105

106

107 **RESULTS**

108 **Octoploid and Diploid R-genes**

109 The genomes of octoploid ‘Camarosa’, diploid *F. vesca*, and diploid *F. innumae* were analyzed
110 for R-gene signatures. The *F. innumae* genome was selected to represent the closely-related ‘old
111 world’ diploid ancestors *F. innumae*, *F. nipponica* and *F. viridis*, which each have highly similar
112 but fragmented genomic assemblies.

113 Putative R-genes were identified based on protein domain and motif analysis, which identified
114 gene models with traditional NLR-type domains, including coiled coil (CC), Toll Interleukin
115 Receptor-like (TIR), Leucine Rich Repeat (LRR), and Nucleotide Binding - APAF-1 (apoptotic
116 protease-activating factor-1), R proteins and CED-4 (*Caenorhabditis elegans* death-4 protein)
117 (NB-ARC). Gene models with NLR-type domains that are not highly specific to NLR sequences
118 (e.g. LRR domains) were included if there was also supporting evidence of an additional NLR-
119 associated motif. BLAST2GO annotated disease resistance associated genes not meeting these
120 criteria were analyzed manually, leading to the intentional inclusion of many putative Receptor-
121 like Kinase (RLK-type) R-genes in this analysis.

122 Octoploid *F. ×ananassa* ‘Camarosa’ carries 1,962 putative resistance genes (1.82% of all genes),
123 including 975 complete or truncated NLR genes (Table 1). NLR gene content is similar in genic
124 proportion to the 367 complete or truncated NLR genes in *F. vesca* (1.09% of all genes) and 387
125 in *F. innumae* (0.5% of all genes) (Table 1). Traditional NLR domains including Coiled Coil (CC),
126 Toll Interleukin Receptor-like (TIR), Leucine Rich Repeat (LRR), and Nucleotide Binding -
127 APAF-1 (apoptotic protease-activating factor-1), R proteins and CED-4 (*Caenorhabditis*
128 *elegans* death-4 protein) (NB-ARC) domains comprise the majority of domain classes in all
129 predicted resistance gene models in diploid and octoploid strawberry accessions (Figure 1). In
130 many categories, the three genomes show somewhat dissimilar ratios of relative NLR-subtype
131 content (Table 1). These include biases towards TIR-only proteins in *F. vesca* and CNL-type R-
132 genes in *F. innumae*. Octoploid ‘Camarosa’ is proportionally intermediate for many NLR
133 categories, relative to *F. vesca* and *F. innumae*. A high proportion of TIR-NB and TIR-NB-LRR-
134 type NLR-genes is observed in ‘Camarosa’. However, the overall proportion of TIR-containing
135 genes is similar. The Resistance to Powdery Mildew 8 (RPW8) domain, a disease resistance
136 domain associated with broad-spectrum mildew resistance in Arabidopsis, appears frequently in
137 strawberry and is present in 136 (13.9%) of octoploid NLRs (Table 1). Basic trends in NLR-

138 subtype genomic content in ‘Camarosa’ does not more strongly resemble either *F. vesca* or *F.*
139 *innumae*.

140 In ‘Camarosa’, 750 genes contain at least one NB-ARC domain, which is the most
141 characteristic domain of NLR-type R-genes (Table 1). The ratio of ‘Camarosa’ NB-ARC-
142 containing genes to total predicted gene content (1:144) is higher than in *F. vesca* (1:171) and *F.*
143 *innumae* (1:262), possibly indicating diversifying selection of NLR genes in octoploid *F.*
144 *×ananassa*. A substantial number of atypical domains are present on strawberry R-genes, including
145 malectin-like carbohydrate-binding domains, RNA-binding domains, transcription factor-like
146 WRKY and F-box domains, and several types of protein kinase domains (Figure 1).

147 Tandem clusters of R-genes were observed in all three of the analyzed strawberry genomes.
148 The phenomena of R-gene expansion through tandem duplication is exemplified in the RPW8-
149 containing R-gene class. Of the seventy-one RPW-containing R-genes in *F. vesca*, all but seven
150 reside in one of a few genomic clusters (Figure S1). The major RPW cluster observed in *F. vesca*
151 chromosome 1 is strongly retained in ‘Camarosa’ (Figure S2). Similar R-gene hotspots are
152 observed throughout the diploid and octoploid strawberry reference genomes. Genome annotations
153 for all NLR domains in ‘Camarosa’ and *F. vesca* genotype Hawaii 4 v2.0 (Tennessee *et al.*, 2014)
154 are provided in File S1. Annotations are also available on the JBrowse web-based genome browser
155 at the Genome Database for the Rosaceae (www.rosaceae.org).

156 **Phylogenetic Analysis of Strawberry R-genes**

157 The conserved NB-ARC domains from ‘Camarosa’, *F. vesca*, and *F. innumae* were compared via
158 maximum likelihood analysis to examine evolutionary trends among NLR genes. NB-ARCs from
159 all three genomes phylogenetically organized mostly according to their extended R-gene domain
160 structures, with TNLs, CNLs, and RPW-associated NB-ARCs forming clades based on this criteria
161 (Figure 2). Minor NLR subtypes, such as WRKY-associated NLR genes, also sorted into a unique
162 subclade based only on NB-ARC sequence. Multiple distinct clades with identical domain
163 architectures were detected, and in a few cases these subclades are relatively distant from one
164 another.

165 **R-gene Transcript Accumulation**

166 Raw RNAseq expression data from different tissues of ‘Camarosa’, derived from the octoploid
167 strawberry gene expression atlas (Sánchez-Sevilla *et al.*, 2017), were reassembled based on the

168 ‘Camarosa’ genome. A majority of ‘Camarosa’ NLR genes are predominantly expressed in the
169 roots and leaves (Figure 3A-B). Comparatively few NLRs are predominantly or specifically
170 expressed in the mature receptacle. Most NLR type R-genes are broadly specific to only one or
171 two tissues. Expressed NLR genes from root, leaf, green and white receptacles show remarkably
172 poor overlap. Overall NLR transcript accumulation is correlated across all stages of receptacle
173 development, with strongest expression in the earlier stages and decreasing with maturity in both
174 the receptacle and achene. Complete R-gene expression values for each tissue are provided in
175 Table S1.

176 Mature receptacle transcriptomes from 61 field-grown individuals of three octoploid populations
177 reveal broadly stable R-gene expression levels (SD 0.09). R-genes comprise 1.8% of the predicted
178 gene models in the ‘Camarosa’ genome, but represent an average of only 0.48% of total transcripts
179 in the mature receptacle (Figure 3C). Minute but statistically significant absolute differences were
180 observed between each of the three populations [$F(2,59) = 19.06, p < .00001$]. To explore possible
181 biases in the gene expression analysis caused by confounding environmental factors, principal
182 component analysis (PCA) was performed on all RNAseq assemblies including two replicates of
183 ‘Mara des Bois’ fruit harvested in different seasons (Figure S2). Total transcript-accumulation
184 variation clusters most strongly according to familial relationship, with the ‘Mara des Bois’
185 replicates showing similar expression patterns. A measured amount of variation due to
186 environmental influence can also be seen, as the two ‘Mara des Bois’ RNAseq replicates cluster
187 somewhat more closely with their co-harvested progeny.

188 **R-gene eQTL in 61 Strawberry Fruit Transcriptomes**

189 eQTL analysis was performed to evaluate heritable genotypic effects on R-gene transcription using
190 61 octoploid IStraw35 genotypes and mature fruit transcriptomes. This analysis identified 77 R-
191 gene-like sequences with at least one highly-significant locus explaining differential expression
192 (3.9% of octoploid genome-predicted R-genes). These R-genes include 53 NB-ARC containing
193 genes, comprised of 25 TNL’s, 14 CNL’s, 3 NBS-RPW proteins, and 11 NB-ARC-only proteins
194 (File S1). The majority of remaining eQTL genes are TIR, LRR, and RPW-only genes. As the
195 ‘Camarosa’ genomic locus of each transcript is known, *cis* vs *trans* eQTL status was determined.
196 Of 77 significant R-gene eQTL transcripts, all 77 R-genes are regulated via a *cis*-genetic locus
197 (Table 2), of which 24 R-genes are also under regulation of an additional second *trans*-eQTL
198 (Table 3). No solely *trans*-eQTL were discovered among this set of R-genes. The most significant

199 IStraw35 SNP marker name and position for each R-gene transcript is provided with the eQTL
200 phase, minor allele frequency, p-value (FDR-adjusted), heritability estimate, expression in parental
201 lines, and BLAST2GO description.

202 A representative eQTL R-gene (maker-Fvb5-1-snap-gene-191.37) is detailed in Figure 6. Analysis
203 by BLAST2GO indicates an “RPM1-like disease resistance gene” whose *Arabidopsis thaliana*
204 homolog confers resistance to *Pseudomonas syringae*. This gene is hereafter referred to as
205 “*FaRPM1.1*”. An unusual double NB-ARC structure is predicted for *FaRPM1.1* (Figure 6A). An
206 eQTL was detected for this gene relative to chromosome 5 on the *F. vesca* genome position (Figure
207 6B). This eQTL is superficially analogous to the physical position of octoploid *FaRPM1.1* on
208 chromosome 5, homoeolog 1 (Figure 6C). The significant eQTL markers are not included in the
209 ‘Holiday’ × ‘Korona’ octoploid genetic map, impeding a recombination-based subgenomic genetic
210 association (van Dijk *et al.*, 2014). However, the associated marker physical sequences match
211 uniquely to the ‘Camarosa’ chromosome 5 homoeolog 1 locus, within several kilobases of the
212 *FaRPM1.1*, confirming a *cis*-eQTL designation (Figure 6D).

213 **Evolutionary Pressure on *F. ×ananassa* R-genes**

214 Elevated median *dN/dS* ratios were observed across all 1,962 predicted *F. ×ananassa* R-genes
215 (0.4232) compared to non R-genes (0.3526) (Figure 4). Fewer R-genes exhibited extremely low
216 *dN/dS* ratios, indicating that high degrees of R-gene conservation are less common. However, a
217 similar rate of hypervariable genes (*dN* >> *dS*) was observed between R-genes and non R-genes. A
218 complete list of *dN/dS* ratios for each *F. ×ananassa* R-gene is provided in Supplementary Table
219 1.

220 R-gene *dN/dS* values were compared against transcript accumulation across various strawberry
221 tissues and receptacle stages. R-genes with low transcript accumulation across all tissues were
222 correlated with higher *dN/dS* ratios (Pearson’s *r* = -0.69, *p* < .0001) (Figure S5). In other words,
223 R-genes with poor evidence of expression also have higher ratios of non-synonymous mutation
224 capable of altering amino acid sequences and affecting protein function.

225 **Subgenome Dominance in Octoploid Strawberry**

226 Polyploidization is associated with rapid genome remodeling events to establish a new
227 homeostasis, including selective gene loss and methylation. While R-gene expansiveness is often
228 considered evolutionarily favorable, genes that are stoichiometrically or dosage sensitive are more

229 commonly retained in duplicate after polyploidization (Edger and Pires, 2009, Birchler and Veitia,
230 2012, Edger *et al.*, 2017a). The ‘Camarosa’ octoploid genome, in comparison with the genomes
231 from its diploid *F. vesca*-like and *F. iinumae*-like ancestors, has provided an ideal platform to
232 study the general biological phenomena of post-hybridization genome remodeling and subgenome
233 dominance (Edger *et al.*, 2019). To gauge R-gene post-hybridization retention specifically, a gene-
234 focused baseline assessment of subgenome dominance in the ‘Camarosa’ octoploid genome was
235 necessary. Putative gene ancestry was predicted based on gene-by-gene sequence comparisons to
236 determine the closest ‘Camarosa’ gene homologs in *F. vesca* (*Fragaria_vesca_v2.0.a2.cds*) and *F.*
237 *iinumae* (*FII_r1.1.cds*), which is representative of the highly similar ‘old world’ subgenomes. This
238 gene-by-gene putative orthology analysis was selected over a total comparison of homeologous
239 chromosomes, as extensive genetic transfer from the *F. vesca*-like subgenome has strongly
240 converted all subgenomes to contain *F. vesca*-like genes over time (Tennesen *et al.*, 2014), and
241 because the *F. iinumae* *FII_r1.1* genome is incompletely assembled and is not amenable to whole-
242 genome alignment. By this facile coding-sequence comparison method, a significant bias towards
243 the retention and/or expansion of *F. vesca*-like genes is observed in the ‘Camarosa’ genome
244 (Figure 5A), with an even stronger bias towards *F. vesca*-like fruit gene expression (Figure 5B)
245 consistent with previous analyses (Edger *et al.*, 2019). Of 108,087 *F. ×ananassa* ‘Camarosa’
246 predicted gene models, 68,664 genes (63.5%) were most similar to an *F. vesca* gene model, with
247 35,377 (32.7%) most similar to an *F. iinumae* gene model, with a minority of genes not closely
248 matching either. A single homoeologous chromosome with significantly more *F. vesca*-like genes
249 (~80% *F. vesca*-like) was seen in every chromosomal group. In a majority of cases, this putative
250 *F. vesca*-derived chromosome possesses the greatest total gene content of the chromosome group.
251 In 61 fruit transcriptomes, 73.7% of total transcripts derived from a gene sequence most similar to
252 *F. vesca*, corresponding to a 10.2% expression increase relative to the baseline genomic retention
253 bias. This bias towards the expression of *F. vesca*-like sequences was seen on every subgenome
254 (Figure 5B, yellow highlight).

255 **NLR-gene Subgenome Dominance**

256 Significant gene retention bias towards R-genes that are more *F. vesca*-like is observed in
257 ‘Camarosa’ gene models (Figure 6). Of the 750 predicted NLR-gene models, 71.7% more closely
258 resemble a *F. vesca* gene rather than an *F. iinumae* gene (Figure 6A). This is somewhat higher
259 than the baseline retention bias towards *F. vesca*-like genes in octoploid (63.8%) from this

260 analysis. In every chromosome group, the *F. vesca*-like homoeologous chromosomes (yellow
261 highlight) retained the greatest number of NLRs. Of expressed R-genes, 1,125 demonstrate the
262 highest sequence identity with an *F. vesca* gene, 444 show highest sequence identity with an *F.*
263 *iinumae* gene, and 2 (an RPW-only gene, and an LRR_8-only gene) are without significant
264 matches to either diploid genome. While *F. vesca*-like genes contribute the most to total mature
265 fruit NLR expression (70.5% of transcripts), this is proportional to *F. vesca*-like NLR genome
266 content (71.3%) and is similar in magnitude to general *F. vesca* expression bias (73.7%) (Figure
267 6B). In other words, *F. vesca*-like NLR genes are retained in the octoploid genome somewhat
268 above the baseline bias, but do not experience the additional expression bias that is a generic
269 feature of *F. vesca*-like transcripts.

270 **RenSeq for Strawberry Resistance Genes**

271 A panel of sequence capture probes was designed based on putative R-gene sequences discovered
272 in the genomes of *F. ×ananassa* ‘Camarosa’, *F. vesca* genotype Hawaii 4, *F. iinumae*, and de novo
273 fruit transcriptomes from *F. ×ananassa* cultivars ‘Mara des Bois’ and ‘Florida Elyana’. Benchtop
274 RenSeq capture on genomic DNA was performed on a collection of sixteen strawberry genotypes,
275 including twelve *F. ×ananassa* advanced breeding selections, three *F. ×ananassa* disease-resistant
276 cultivars, and a diploid *F. vesca*. As a preliminary validation of capture efficiency with this novel
277 RenSeq probe panel, multiplexed Illumina sequencing was performed on captured R-gene
278 genomic libraries. An average of 2.60 million reads ($2 \times 100\text{bp}$) was obtained for each of sixteen
279 libraries from a single lane. Reads from octoploid and diploid lines were mapped to their respective
280 annotated genomic references. An average R-gene resequencing depth of 26x was achieved in the
281 ‘Camarosa’ RenSeq line and 30x in the *F. vesca*, with similar coverage ranges in the other diverse
282 octoploid accessions (Figure 8). In the ‘Camarosa’ RenSeq line, 68% of reads mapped to an
283 annotated resistance gene, while an additional 20% of reads mapped to a non-R-gene gene model.
284 In *F. vesca* this efficiency was lower, where 36% of reads mapped to an annotated R-gene. A
285 FASTA of RenSeq probes is provided for use in File S2. Example probe coverage is detailed in
286 Figure S6.

287

288 **DISCUSSION**

289 These results provide a characterization of the R-gene complement of cultivated octoploid
290 strawberry and the relationship to the extant diploid relatives, *F. vesca* and *F. innumae*.
291 Commercial strawberry is hypothesized to contain a single *F. vesca*-like subgenome, and three
292 highly-similar ‘old world’ subgenomes which are likely derived from *F. innumae*, *F. viridis*, and
293 *F. nipponica* (Edger *et al.*, 2019). Polyploidization is associated with massive genome remodeling
294 events including gene loss (Edger *et al.*, 2017a, Edger *et al.*, 2018). Linkage-map comparisons in
295 octoploid and diploid strawberry have uncovered extensive unidirectional homoeologous
296 exchanges which have broadly converted the three ‘old world’ *F. innumae*-like subgenomes to be
297 more *F. vesca*-like (Tennessen *et al.*, 2014). This finding explains the difficulties of clear ancestral
298 delineation of strawberry homoeologs (Vining *et al.*, 2017). Recent analysis of the octoploid
299 genome reveals that biased homologous exchanges have converted other subgenomes to be more
300 like the dominant *F. vesca*-like subgenome (Edger *et al.*, 2019). The present gene-level homology
301 and expression analysis shows the majority of *F. vesca*-like dominance is derived from *F. vesca*-
302 like genes residing on alternate subgenomes. For NLR genes in particular, the bias towards *F.*
303 *vesca*-like genomic retention was more pronounced. Unlike general octoploid genes, expression
304 of *F. vesca*-like and *F. innumae*-like NLRs is proportional to their genomic representation. This
305 finding provides potential insight into the practical drivers of subgenome conversion.
306 Consolidation of redundant genes and maintenance of stoichiometrically sensitive genes has been
307 hypothesized as a driver for gene retention bias. NLRs are involved in consequential and sensitive
308 protein-level interactions, including signaling functions requiring homo- and hetero-dimerizations.
309 Avoidance of dysfunctional NLR molecular interactions may have contributed to the observed
310 biases in NLR retention and expression, post-polyploidization.

311 Multiple distinct NLR clades with identical domain architectures were detected, likely
312 distinguishing intra-subgenome homologs from different subgenomes. These likely reflect broad
313 ancestral sequence divergences prior to hybridization. Comparison of R-genes in octoploid and
314 diploid strawberry reveals enrichment of different subtypes. The ‘Camarosa’ genome shows a
315 large increase in complete TNL-type R-genes and a concomitant decrease in truncated TIR-only
316 genes, relative to its diploid ancestral relatives. The *F. innumae* genome shows a considerably
317 larger amount of CNL-types. TNLs have been nearly eliminated from most monocot genomes in
318 bias towards CNL-types (Nepal *et al.*, 2017). The reasons for emerging divisions in TNL/CNL

319 content in plant genomes remains unclear. In hybrid *F. ×ananassa*, it is possible that relatively
320 high number of complete TNL genes is a result of higher rate of retention post-polyploidization in
321 this category. Many of the non-classical domains discovered in ‘Camarosa’ R-genes have also
322 been found and characterized in the R-genes of other species. These include an LRR/Malectin-like
323 RLK protein, which mediates powdery mildew resistance in barley and wheat (Rajaraman *et al.*,
324 2016). Atypical R-gene domains physically associated with NB-ARCs have been implicated in a
325 variety of active disease resistance functions, including signal transduction and defense gene
326 activation, and serving as decoy endogenous sequences to bait pathogen effectors into direct
327 interaction and detection (Khan *et al.*, 2016).

328 A large proportion of strawberry NLR genes from octoploid and diploid genomes are associated
329 with RPW8 domains. It has been suggested that the RPW8 domain emerged with the earliest land
330 plants and subsequently merged with NLR genes, however their prevalence across plant genomes
331 varies widely (Zhong and Cheng, 2016). The RPW domain appears to have been completely lost
332 in monocots, and is rare in many other species. R-gene genomic studies frequently neglect to assess
333 the presence of NLR-associated RPW domains. Two NBS-RPW8 proteins conferring mildew-
334 resistance have been described in the *Arabidopsis thaliana* genome (Xiao *et al.*, 2001) that retained
335 their function when expressed in grape (Hu *et al.*, 2018). The *AtRPW8.2* gene was recently shown
336 to induce the expression of defense-related genes when expressed in strawberry leaves (Cui *et al.*,
337 2017). This R-gene subtype has apparently expanded in strawberry, possibly due to unusually high
338 mildew disease pressure exerted on strawberry species and intense selection for resistance.
339 However, R-gene domain content is not reliably predictive of resistance specificity, and close R-
340 gene paralogs are known to confer resistance to pathogens in entirely different kingdoms (Wen *et*
341 *al.*, 2015). Interestingly, the strawberry RPW8 domain is frequently found in association with NB-
342 ARC-containing genes but never with TIRs. The purpose of RPW8 gene expansion in strawberry
343 remains an interesting open question.

344 Octoploid NLR transcript accumulation is low throughout the strawberry plant, but is particularly
345 low in the mature receptacle. This is a somewhat unexpected result due to the many pathogens
346 targeting this susceptible organ. It is possible that only certain R genes are highly upregulated in
347 the response to pathogen attack. Another possibility is that resistance based on the hypersensitive
348 response may be less effective at mature stages, where cell wall disruption has already initiated
349 with ripening and the intercellular environment is conducive to pathogen growth. Transcriptional

350 response to *Botrytis cinerea* infection in the mature octoploid receptacle led to differential
351 expression of over 1,500 genes, including secondary metabolism and pathogenesis-related (PR)
352 genes, but only 15 NLR genes (Xiong *et al.*, 2018). In the present study, elevated NLR
353 transcription in the green, white, and turning stages suggest NLR-based resistance may be more
354 prevalent at these earlier developmental stages. The highest levels of NLR expression were seen
355 in the roots and leaves, indicating this mode of resistance may be more common in these tissues.
356 NLR expression overlaps poorly between tissues, supporting the concept that NLRs are optimized
357 for each tissue. It would be interesting to examine the patterns of tissue specific expression of R-
358 genes against different strawberry pathogens.

359 The genetics of differential fruit expression of R-genes in strawberry cultivars was examined via
360 eQTL analysis. In many cases, the identified genetic markers described presence/absence of R-
361 gene expression. The identified eQTLs were often due to a *cis* variant at a single detectable locus,
362 very close to the physical position of the gene itself. This is suggestive of a mutation in a *cis*-
363 regulatory element, such as the gene promoter or 5'-UTR, or a genic presence/absence structural
364 variation. Such presence/absence variation affects nearly 20% of genes in the *Brassica oleracea*
365 pangenome and is a major contributor of agronomic trait diversity (Golicz *et al.*, 2016). As these
366 strawberry R-gene eQTL are derived from crosses of cultivars with differing ranges of pathogen
367 susceptibility, these eQTL genes represent strong candidates for functional disease resistance and
368 potential genetic improvement. These disclosed R-gene eQTL marker sequences may be cross-
369 referenced with existing disease-resistance QTL to potentially identify causal R-genes. As
370 categories of R-genes are expressed at very low levels unless induced by pathogens (Lai and
371 Eulgem, 2017), the genotype \times pathogen interaction may have lowered confidence values or
372 introduced possible type II errors in eQTL detection. However, the reproducibility of *cis*-eQTL
373 tends to be particularly high in related populations (Peirce *et al.*, 2006). Additional replicates and
374 infected/non-infected challenge conditions will likely reveal additional eQTL associations and
375 greatly improve the confidence of heritability estimates, and may be used to validate pathogen-
376 induced R-gene candidates.

377 *F. xananassa* predicted R-genes (NLRs and other R-gene types) have elevated average *dN/dS*
378 ratios compared to non R-genes, indicating greater overall tendency towards divergent selection.
379 R-genes with very low *dN/dS* ratios are likely to be conserved disease resistance genes. This active
380 evolutionary selection is highly indicative of function. Of particular interest are strawberry R-

381 genes demonstrating both low dN/dS values and low transcript levels across all tissues (Table S1).
382 Many functional R-genes are expressed at low levels, either constitutively or until elicited by the
383 proper pathogen (Lai and Eulgem, 2017). Such R-genes may be difficult to distinguish from
384 pseudogenes on a purely transcriptional bases. Low dN/dS values demonstrate selective pressure
385 to maintain these sequences, offering evidence of maintained function despite low expression. The
386 results of this combinatorial analysis can be used help identify novel sources of R-gene-based
387 resistance which may be otherwise difficult to detect. It should be noted that this analysis is
388 performed in the context of a single cultivar, which has undergone several centuries of artificial
389 selection. It is possible that wild octoploid species may reveal different and more natural patterns
390 of disease-resistance selection. More sequenced accessions from geographically diverse wild and
391 cultivated germplasm are needed. Further analysis on the octoploid pangenome will reveal more
392 detailed selection patterns, and more importantly, reveal recent selection sweep events which may
393 have occurred in certain R-gene groups.

394 Many R-genes were discovered clustered in the genomes of both octoploid and diploid strawberry,
395 highlighting the challenges of resolving individual R-genes via association mapping and positional
396 cloning. The difficulty of isolating functional R-genes from strawberry disease resistance QTL
397 was the principle motivator of this analysis. A thorough identification of R-genes in the octoploid
398 genome is necessary for future genomics and genetics analysis in strawberry disease-resistance
399 breeding programs. Additionally, this information is prerequisite for creating a RenSeq probe
400 panel, to facilitate targeted R-gene sequencing in breeding programs.

401 A novel strawberry RenSeq capture-probe library was developed based on the R-gene sequences
402 identified from genomic and transcriptomic resources. This 39,501-probe panel was
403 experimentally validated using octoploid and diploid genomes and resulted in an average $\sim 20\times$ R-
404 gene resequencing depth per genomic library, using only multiplexed short reads. RenSeq
405 assembly in ‘Camarosa’ and the *F. vesca* genotype Hawaii 4 resulted in significant coverage of R-
406 genes. Interestingly, the capture efficiency (R-gene reads over total reads) was somewhat lower in
407 *F. vesca*, likely representing the saturation of capture probes in the smaller *F. vesca* genome.
408 Similar rates of perfect sequence matching along the entire read in ‘Camarosa’ and *F. vesca*
409 (66.24% and 69.68%, respectively) indicates that theoretical octoploid reference sequence errors
410 are not likely promoting RenSeq assembly error in ‘Camarosa’. However, 14.4% of mapped
411 ‘Camarosa’ R-gene reads have an equally valid alternative R-gene mapping locus, compared with

412 just 4.83% in *F. vesca*. This difference indicates that homoeologous sequence redundancy is an
413 appreciable issue for mapping short-reads in polyploids, even with an isogenic (but not haplotype-
414 specific) mapping reference. Longer sequencing read-lengths, spanning less well-conserved non-
415 coding sequences, will assist in de novo resolution of similar loci in octoploid strawberry.
416 Combining RenSeq with longer-read third generation sequencing technologies will allow for
417 improved de novo assembly of R-gene loci, and will greatly facilitate causal mutation detection
418 within disease resistance QTL in octoploid strawberry.

419

420

421 **MATERIALS AND METHODS**

422 **Plant Populations and Genetic Materials**

423 Three pedigree-connected and segregating strawberry populations were created from crosses
424 ‘Florida Elyana’ × ‘Mara de Bois’, ‘Florida Radiance’ × ‘Mara des Bois’, and ‘Strawberry
425 Festival’ × ‘Winter Dawn’ (Figure S7). These cultivars and 54 progeny were selected for RNAseq
426 and IStraw35 SNP genotyping analysis (Verma *et al.*, 2017), and were used to identify expressed
427 genes and R-gene eQTL. De novo assemblies of ‘Mara des Bois’ and ‘Florida Elyana’ were also
428 used to help design RenSeq capture probes.

429 For RenSeq, 14 disease resistant octoploid cultivars and elite breeding lines were selected from
430 the University of Florida breeding program, and supplemented with ‘Camarosa’ and with the
431 ancestral diploid *F. vesca*. The RenSeq lines are *F. vesca* genotype Hawaii 4, ‘Camarosa’, Sweet
432 Sensation® ‘Florida127’, ‘Florida Elyana’, 11.28-34, 11.77-96, 11.98-41, 12.115-10, 12.121-5,
433 13.26-134, 13.42-5, 13.55-195, 14.100-58, 14.100-59, 14.101-154, and 14.101-225.

434 **Identification of R-genes in Strawberry spp.**

435 R-genes were predicted from the strawberry octoploid ‘Camarosa’ draft genome
436 “F_ana_Camarosa_6-28-17.rm” (Edger *et al.*, 2019), the diploid *F. vesca* reassembly
437 “Fragaria_vesca_v2.0.a2” (Tenessen *et al.*, 2014), and the diploid *F. innumae* assembly
438 “FII_r1.1” (Hirakawa *et al.*, 2014). Domain-level analysis was performed using the CLC
439 Genomics Workbench 11 HMM implementation to search for Pfam- v29 domains on translated
440 gene models from all genomic and transcriptomic strawberry resources. Motif search was
441 performed on all translated gene models, using 56 R-gene-associated motifs collected from
442 (Lukasik and Takken, 2009, Jupe *et al.*, 2012, Van Ghelder and Esmenjaud, 2016). The CLC
443 Genomics Workbench 11 (CLC Bio, Denmark) pattern discovery tool was trained on a preliminary
444 list of strawberry R-genes, and novel motifs were reiterated back to all protein models. The Ncoils
445 sequence analysis algorithm (Lupas *et al.*, 1991) was used to detect coiled-coil domains, and the
446 output was parsed into GFF3 format for protein list reannotation. BLAST2GO annotation (Conesa
447 *et al.*, 2005) was performed to assign putative functions to all genes and confirm sequence
448 association with disease resistance in a cross-referenced database.

449 Protein models containing canonical R-gene domains (eg. NB-ARC domain) were selected for

450 inclusion as R-genes, as were gene models with more common domains (eg. LRR) with supporting
451 evidence of an R-gene-associated motif. BLAST2GO annotated disease resistance associated
452 genes not meeting the domain and motif-level criteria were analyzed for potential inclusion,
453 leading to the inclusion of many LRR-containing RLK putative R-genes.

454 **NB-ARC Phylogenetic Analysis**

455 NB-ARC domains were extracted from *F. iinumae*, *F. vesca*, and *F. ×ananassa* ‘Camarosa’. The
456 CIPRES Science Gateway (Miller *et al.*, 2010) was utilized for full-length protein sequence
457 alignment using MUSCLE v3.7 (Edgar, 2004) and Maximum likelihood analysis using RAxML
458 v8.2.10 (Stamatakis, 2014). Tree construction was performed using the PROTGAMMA rate
459 distribution model with 100 bootstrap replicates, and rooted with human APAF-1. This process
460 was replicated five times using different random number seeds. Trees were visualized in CLC
461 Genomic Workbench 11 with a 50% threshold bootstrap value. Word clouds were generated per
462 clade based on the relative domain content of the full proteins.

463 **Subgenome Dominance in Octoploid Strawberry R-genes**

464 The closest homolog for each *F. ×ananassa* ‘Camarosa’ gene in either *Fragaria vesca*_v2.0.a2.cds
465 or FII_r1.1.cds was determined via BLAST analysis (e-value threshold < 0.1, word size=25,
466 match=1, mismatch=1, existence=0, extension=2). *F. vesca*-like and *F. iinumae*-like gene counts
467 and TPMs were independently calculated for each octoploid chromosome. This process was
468 performed first on all genes in the ‘Camarosa’ genome to establish the baseline gene retention and
469 expression bias, and then repeated using only predicted NLR genes.

470 **dN/dS Analysis**

471 *dN* and *dS* values were computed using a set of custom scripts
472 (https://github.com/Aeyocca/ka_ks_pipe/). Orthologous genes between the *F. ×ananassa* and *F.*
473 *vesca* v4 (Edger *et al.*, 2017b) genomes were identified using the compara module in JCVI utilities
474 library (Tang *et al.*, 2015). Filtering of the JCVI utilities output was performed using a custom perl
475 script to identify the best syntenic ortholog and best blast hit below e-value 1e-4. Alignment of
476 each orthologous gene pair was performed using MUSCLE v3.8.31 (Edgar, 2004), followed by
477 PAL2NAL (v14) (Suyama *et al.*, 2006) to convert the peptide alignment to a nucleotide alignment.
478 Finally, *dN* and *dS* values were computed between those gene pairs using codeml from PAML
479 Version 4.9h (Yang, 2007) with parameters specified in the control file found in the GitHub

480 repository listed above.

481 **Tissue-specific Transcriptome Analysis**

482 Raw short read RNAseq libraries from various ‘Camarosa’ tissue (Sánchez-Sevilla *et al.*, 2017)
483 with the study reference PRJEB12420 were download from the European Nucleotide Archive
484 (<https://www.ebi.ac.uk/ena>). The complete 54 library RNAseq experiment consisted of six
485 independent green receptacle libraries, six white receptacle libraries, six turning receptacle
486 libraries, six red receptacle libraries, three root libraries, three leaf libraries, and six achene libraries
487 each for all corresponding fruit stages. Raw RNAseq reads were assembled to the ‘Camarosa’
488 reference using the same pipeline as previously described for fruit transcriptome population
489 analysis. Expression values from biologically-replicated libraries were averaged. Clustvis
490 (Metsalu and Vilo, 2015) was used for tissue-based RNAseq clustering and heatmap visualization
491 using correlation distance and average linkage with scaling applied using default parameters.

492 **Fruit Transcriptome Analysis**

493 61 fruit transcriptomes were sequenced via Illumina paired-end RNAseq (Avg. 65million reads,
494 2x100bp), and consisted of parents and progeny from crosses of ‘Florida Elyana’ × ‘Mara de Bois’,
495 ‘Florida Radiance’ × ‘Mara des Bois’, and ‘Strawberry Festival’ × ‘Winter Dawn’. Reads were
496 trimmed and mapped to the *F. ×ananassa* octoploid ‘Camarosa’ annotated genome using CLC
497 Genomic Workbench 11 (mismatch cost of 2, insertion cost of 3, deletion cost of 3, length fraction
498 of 0.8, similarity fraction of 0.8, 1 maximum hit per read). Reads that mapped equally well to more
499 than one locus were discarded from the analysis. RNAseq counts were calculated in Transcripts
500 Per Million (TPM). Three-dimensional principle component analysis (PCA) was performed on all
501 RNAseq assemblies, including two replicates of ‘Mara des Bois’ fruit harvested three years apart
502 and sequenced independently (Figure S2). Transcript abundances were normalized via the Box-
503 Cox transformation algorithm performed in R (R. Development Core Team, 2014) prior to eQTL
504 analysis. The BLAST2GO pipeline was used to annotate the full ‘Camarosa’ predicted gene
505 complement.

506 **Genotyping and Genetic Association of Octoploid Fruit R-genes**

507 The Affymetrix IStraw35 Axiom[®] SNP array (Verma *et al.*, 2017) was used to genotype 60
508 individuals, including six parental lines from three independent biparental RNAseq populations
509 (Figure S7). Sequence variants belonging to the Poly High Resolution (PHR) and No Minor

510 Homozygote (NMH) marker classes were included for association mapping. Mono High
511 Resolution (MHR), Off-Target Variant (OTV), Call Rate Below Threshold (CRBT), and Other
512 marker quality classes, were discarded and not used for mapping. Individual marker calls
513 inconsistent with Mendelian inheritance from parental lines were removed. The *F. vesca* physical
514 map was used to orient marker positions as current octoploid maps do not include a majority of
515 the available IStraw35 markers. A genome-wide analysis study (GWAS) was performed using
516 GAPIT v2 (Tang *et al.*, 2016) performed in R. R-gene eQTL were evaluated for significance based
517 on the presence of multiple co-locating markers of p -value < 0.05 after false discovery rate
518 correction for multiple comparisons. *Cis* vs *trans* eQTL determinations were made by
519 corroborating known ‘Camarosa’ physical gene position with the eQTL position the *F. vesca* map.
520 In the example case of *FaRPM1.1*, subgenomic localization was confirmed via BLAST of the
521 associated markers to the correct ‘Camarosa’ homoeologous chromosome.

522 **RenSeq Probe Design and Validation**

523 A panel of 39,501 of 120mer-length capture probes were designed based on the set of discovered
524 strawberry R-genes from *F. ×ananassa* ‘Camarosa’, *F. vesca* genotype Hawaii 4, *F. iinumae*
525 genomes, and de novo fruit transcriptomes from *F. ×ananassa* ‘Mara des Bois’ and ‘Florida
526 Elyana’. A proprietary algorithm was used to select for capture probes of ideal hybridization
527 thermodynamics and screened for potential off-target capture in the intergenic regions of
528 ‘Camarosa’ and *F. vesca* (Rapid Genomics LLC, Gainesville FL). Probes were designed to not
529 span exon-exon junction, to facilitate cross-utility for both genomic and cDNA libraries (Figure
530 S6). A minimum baseline of 1x probe coverage was provided across the length of every predicted
531 R-gene coding sequence, and additional probes were designed against conserved R-gene domains
532 in order to promote capture of unknown and divergent R-genes across diverse octoploid
533 accessions. RenSeq capture was performed on genomic libraries from fifteen octoploid disease-
534 resistant cultivars and advanced breeding selections, and *F. vesca*, based on conditions set by (Jupe
535 *et al.*, 2014), with optimizations provided by Rapid Genomics LLC. Captured libraries were
536 sequenced via 16x multiplexed Illumina Hiseq (2×100 bp) and mapped to their respective
537 annotated genomic references using CLC Genomic Workbench 11 (CLCBio, Aarhus, Denmark)
538 (Similarity fraction = 0.9, Length fraction = 0.9, Match score = 1, Mismatch cost = 2, Insertion
539 cost = 3, Deletion cost = 3).

540 **Data Availability**

541 Supplementary figures, tables, files, and raw data are available at FigShare. Custom scripts used
542 for performing dN/dS analysis are available at Github: https://github.com/Aeyocca/ka_ks_pipe/.
543 Raw short read RNAseq data from fruit transcriptomes are available from the NCBI Short Read
544 Archive under project SRP039356 (<http://www.ncbi.nlm.nih.gov/sra/?term=SRP039356>). Raw
545 short read RNAseq data from the ‘Camarosa’ gene expression atlas (Sánchez-Sevilla et al., 2017)
546 are available at the European Nucleotide Archive (<https://www.ebi.ac.uk/ena>) with the study
547 reference PRJEB12420. Results derived from these data are compiled in Table S1. File S1 contains
548 BED files for annotating the octoploid genome (Edger *et al.*, 2019) with R-genes and R-gene
549 domains. Renseq probe sequences are provided in File S2. Istraw35 markers, map positions, and
550 sample genotypes used in eQTL analysis are available in File S3.

551

552 ACKNOWLEDGEMENTS

553 We acknowledge Aristotole Koukoulidis for ncoils prediction and annotation, Matthew Robinson
554 for assistance with data normalization, Rapid Genomics LLC for technical assistance in probe
555 generation and sequence capture, Anne Schwartz, Max Hogshead, Kiran Sharma and Nadia
556 Mourad for assistance in data compilation, Ben Harrison and Max Hogshead for assistance in
557 gDNA isolation of eQTL lines, and Dr. Alan Chambers and Dr. Jeremy Pillet for RNA isolation
558 and RNAseq line selection.

559 CONFLICT OF INTEREST

560 The authors declare no conflicts of interest.

561

562 LITERATURE CITED

- 563 **Amil-Ruiz, F., Departamento de Bioquímica y Biología Molecular e Instituto Andaluz de Biotecnología,**
564 **C.d.E.I.A.C.C.d.R.E.S.O.U.d.C.C.S., Blanco-Portales, R., Muñoz-Blanco, J. and Caballero, J.L.** (2018)
565 The Strawberry Plant Defense Mechanism: A Molecular Review. *Plant and Cell Physiology*, **52**, 1873-
566 190310.1093/pcp/pcr136.
- 567 **Anciro, A., Mangandi, J., Verma, S., Peres, N., Whitaker, V.M. and Lee, S.** (2018) FaRCg1: a quantitative trait
568 locus conferring resistance to Colletotrichum crown rot caused by Colletotrichum gloeosporioides in
569 octoploid strawberry. *Theoretical and Applied Genetics*10.1007/s00122-018-3145-z.
- 570 **Andolfo, G., Jupe, F., Witek, K., Etherington, G.J., Ercolano, M.R. and Jones, J.D.G.** (2014) Defining the full
571 tomato NB-LRR resistance gene repertoire using genomic and cDNA RenSeq. *BMC Plant Biology*, **14**,
572 12010.1186/1471-2229-14-120.
- 573 **Arya, P., Kumar, G., Acharya, V. and Singh, A.K.** (2014) Genome-Wide Identification and Expression Analysis
574 of NBS-Encoding Genes in Malus x domestica and Expansion of NBS Genes Family in Rosaceae. *PLOS*
575 *ONE*, **9**, e10798710.1371/journal.pone.0107987.
- 576 **Baumgartner, I.O., Patocchi, A., Frey, J.E., Peil, A. and Kellerhals, M.** (2015) Breeding Elite Lines of Apple

- 577 Carrying Pyramided Homozygous Resistance Genes Against Apple Scab and Resistance Against Powdery
578 Mildew and Fire Blight. *Plant Molecular Biology Reporter*, **33**, 1573-158310.1007/s11105-015-0858-x.
- 579 **Birchler, J.A. and Veitia, R.A.** (2012) Gene balance hypothesis: Connecting issues of dosage sensitivity across
580 biological disciplines. *Proceedings of the National Academy of Sciences*, **109**,
581 1474610.1073/pnas.1207726109.
- 582 **Conesa, A., Götz, S., García-Gómez, J.M., Terol, J., Talón, M. and Robles, M.** (2005) Blast2GO: a universal tool
583 for annotation, visualization and analysis in functional genomics research. *Bioinformatics*, **21**, 3674-
584 367610.1093/bioinformatics/bti610.
- 585 **Cordova, L.G., Amiri, A. and Peres, N.A.** (2017) Effectiveness of fungicide treatments following the Strawberry
586 Advisory System for control of Botrytis fruit rot in Florida. *Crop Protection*, **100**, 163-
587 167<https://doi.org/10.1016/j.cropro.2017.07.002>.
- 588 **Cui, M.-Y., Wei, W., Gao, K., Xie, Y.-G., Guo, Y. and Feng, J.-Y.** (2017) A rapid and efficient Agrobacterium-
589 mediated transient gene expression system for strawberry leaves and the study of disease resistance proteins.
590 *Plant Cell, Tissue and Organ Culture (PCTOC)*, **131**, 233-24610.1007/s11240-017-1279-3.
- 591 **Djian-Caporalino, C., Palloix, A., Fazari, A., Marteu, N., Barbary, A., Abad, P., Sage-Palloix, A.-M., Mateille,
592 T., Risso, S., Lanza, R., Taussig, C. and Castagnone-Sereno, P.** (2014) Pyramiding, alternating or mixing:
593 comparative performances of deployment strategies of nematode resistance genes to promote plant resistance
594 efficiency and durability. *BMC Plant Biology*, **14**, 5310.1186/1471-2229-14-53.
- 595 **Edgar, R.C.** (2004) MUSCLE: multiple sequence alignment with high accuracy and high throughput. *Nucleic acids
596 research*, **32**, 1792-1797
- 597 **Edger, P.P., McKain, M.R., Bird, K.A. and VanBuren, R.** (2018) Subgenome assignment in allopolyploids:
598 challenges and future directions. *Current Opinion in Plant Biology*, **42**, 76-
599 80<https://doi.org/10.1016/j.pbi.2018.03.006>.
- 600 **Edger, P.P. and Pires, J.C.** (2009) Gene and genome duplications: the impact of dosage-sensitivity on the fate of
601 nuclear genes. *Chromosome Research*, **17**, 69910.1007/s10577-009-9055-9.
- 602 **Edger, P.P., Poorten, T.J., VanBuren, R., Hardigan, M.A., Colle, M., McKain, M.R., Smith, R.D., Teresi, S.J.,
603 Nelson, A.D.L., Wai, C.M., Alger, E.I., Bird, K.A., Yocca, A.E., Pumplun, N., Ou, S., Ben-Zvi, G., Brodt,
604 A., Baruch, K., Swale, T., Shiue, L., Acharya, C.B., Cole, G.S., Mower, J.P., Childs, K.L., Jiang, N.,
605 Lyons, E., Freeling, M., Puzey, J.R. and Knapp, S.J.** (2019) Origin and evolution of the octoploid
606 strawberry genome. *Nature Genetics*, **51**, 541-54710.1038/s41588-019-0356-4.
- 607 **Edger, P.P., Smith, R., McKain, M.R., Cooley, A.M., Vallejo-Marin, M., Yuan, Y., Bewick, A.J., Ji, L., Platts,
608 A.E., Bowman, M.J., Childs, K.L., Washburn, J.D., Schmitz, R.J., Smith, G.D., Pires, J.C. and Puzey,
609 J.R.** (2017a) Subgenome Dominance in an Interspecific Hybrid, Synthetic Allopolyploid, and a 140-Year-
610 Old Naturally Established Neo-Allopolyploid Monkeyflower. *The Plant Cell*, **29**, 2150
- 611 **Edger, P.P., VanBuren, R., Colle, M., Poorten, T.J., Wai, C.M., Niederhuth, C.E., Alger, E.I., Ou, S., Acharya,
612 C.B., Wang, J., Callow, P., McKain, M.R., Shi, J., Collier, C., Xiong, Z., Mower, J.P., Slovin, J.P.,
613 Hytönen, T., Jiang, N., Childs, K.L. and Knapp, S.J.** (2017b) Single-molecule sequencing and optical
614 mapping yields an improved genome of woodland strawberry (*Fragaria vesca*) with chromosome-scale
615 contiguity. *GigaScience*, 710.1093/gigascience/gix124.
- 616 **Farzaneh, M., Kiani, H., Sharifi, R., Reisi, M. and Hadian, J.** (2015) Chemical composition and antifungal effects
617 of three species of Satureja (*S. hortensis*, *S. spicigera*, and *S. khuzistanica*) essential oils on the main
618 pathogens of strawberry fruit. *Postharvest Biology and Technology*, **109**, 145-
619 151<https://doi.org/10.1016/j.postharvbio.2015.06.014>.
- 620 **Funk, A., Galewski, P. and McGrath, J.M.** (2018) Nucleotide-binding resistance gene signatures in sugar beet,
621 insights from a new reference genome. *The Plant Journal*, **95**, 659-67110.1111/tpj.13977.
- 622 **Golicz, A.A., Bayer, P.E., Barker, G.C., Edger, P.P., Kim, H., Martinez, P.A., Chan, C.K.K., Severn-Ellis, A.,
623 McCombie, W.R., Parkin, I.A.P., Paterson, A.H., Pires, J.C., Sharpe, A.G., Tang, H., Teakle, G.R.,
624 Town, C.D., Batley, J. and Edwards, D.** (2016) The pangenome of an agronomically important crop plant
625 Brassica oleracea. *Nature Communications*, **7**, 1339010.1038/ncomms13390
626 <https://www.nature.com/articles/ncomms13390#supplementary-information>.
- 627 **Hammond-Kosack, K.E. and Jones, J.D.G.** (1997) Plant Disease Resistance Genes. *Annual Review of Plant
628 Physiology and Plant Molecular Biology*, **48**, 575-60710.1146/annurev.arplant.48.1.575.
- 629 **Herrington, M.E., Hardner, C., Wegener, M., Woolcock, L.L. and Dieters, M.J.** (2011) Rain Damage to
630 Strawberries Grown in Southeast Queensland: Evaluation and Genetic Control. *HortScience*, **46**, 832-837

- 631 **Hirakawa, H., Shirasawa, K., Kosugi, S., Tashiro, K., Nakayama, S., Yamada, M., Kohara, M., Watanabe, A.,**
632 **Kishida, Y., Fujishiro, T., Tsuruoka, H., Minami, C., Sasamoto, S., Kato, M., Nanri, K., Komaki, A.,**
633 **Yanagi, T., Guoxin, Q., Maeda, F., Ishikawa, M., Kuhara, S., Sato, S., Tabata, S. and Isobe, S.N.** (2014)
634 Dissection of the Octoploid Strawberry Genome by Deep Sequencing of the Genomes of *Fragaria* Species.
635 *DNA Research*, **21**, 169-18110.1093/dnares/dst049.
- 636 **Hu, Y., Li, Y., Hou, F., Wan, D., Cheng, Y., Han, Y., Gao, Y., Liu, J., Guo, Y., Xiao, S., Wang, Y. and Wen, Y.-**
637 **Q.** (2018) Ectopic expression of Arabidopsis broad-spectrum resistance gene RPW8.2 improves the
638 resistance to powdery mildew in grapevine (*Vitis vinifera*). *Plant Science*, **267**, 20-
639 [31https://doi.org/10.1016/j.plantsci.2017.11.005](https://doi.org/10.1016/j.plantsci.2017.11.005).
- 640 **Jia, Y., Yuan, Y., Zhang, Y., Yang, S. and Zhang, X.** (2015) Extreme expansion of NBS-encoding genes in
641 Rosaceae. *BMC Genetics*, **16**, 4810.1186/s12863-015-0208-x.
- 642 **Jupe, F., Chen, X., Verweij, W., Witek, K., Jones, J.D.G. and Hein, I.** (2014) Genomic DNA Library Preparation
643 for Resistance Gene Enrichment and Sequencing (RenSeq) in Plants. In *Plant-Pathogen Interactions:*
644 *Methods and Protocols* (Birch, P., Jones, J.T. and Bos, J.I.B. eds). Totowa, NJ: Humana Press, pp. 291-303.
- 645 **Jupe, F., Pritchard, L., Etherington, G.J., MacKenzie, K., Cock, P.J.A., Wright, F., Sharma, S.K., Bolser, D.,**
646 **Bryan, G.J., Jones, J.D.G. and Hein, I.** (2012) Identification and localisation of the NB-LRR gene family
647 within the potato genome. *BMC Genomics*, **13**, 7510.1186/1471-2164-13-75.
- 648 **Khan, M., Subramaniam, R. and Desveaux, D.** (2016) Of guards, decoys, baits and traps: pathogen perception in
649 plants by type III effector sensors - ScienceDirect. *Current Opinion in Microbiology*, **29**, 49-
650 5510.1016/j.mib.2015.10.006.
- 651 **Lai, Y. and Eulgem, T.** (2017) Transcript-level expression control of plant NLR genes. *Molecular Plant Pathology*,
652 **19**, 1267-128110.1111/mpp.12607.
- 653 **Lukasik, E. and Takken, F.L.W.** (2009) STANDING strong, resistance proteins instigators of plant defence. *Current*
654 *opinion in plant biology*, **12**, 427-436
- 655 **Lupas, A., Van Dyke, M. and Stock, J.** (1991) Predicting Coiled Coils from Protein Sequences. *Science*, **252**, 1162-
656 1164
- 657 **Mangandi, J., Verma, S., Osorio, L., Peres, N.A., van de Weg, E. and Whitaker, V.M.** (2017) Pedigree-Based
658 Analysis in a Multiparental Population of Octoploid Strawberry Reveals QTL Alleles Conferring Resistance to
659 *Phytophthora cactorum*. *G3: Genes/Genomes/Genetics*, **7**, 1707
- 660 **Metsalu, T. and Vilo, J.** (2015) ClustVis: a web tool for visualizing clustering of multivariate data using Principal
661 Component Analysis and heatmap. *Nucleic Acids Research*, **43**, W566-W57010.1093/nar/gkv468.
- 662 **Miller, M.A., Pfeiffer, W. and Schwartz, T.** (2010) Creating the CIPRES Science Gateway for inference of large
663 phylogenetic trees. In *2010 Gateway Computing Environments Workshop (GCE)*, pp. 1-8.
- 664 **Nepal, M.P.A., E. J., Neupane, S. and Benson, B.V.** (2017) Comparative Genomics of Non-TNL Disease Resistance
665 Genes from Six Plant Species. In *Genes (Basel)*.
- 666 **Peirce, J.L., Li, H., Wang, J., Manly, K.F., Hitzemann, R.J., Belknap, J.K., Rosen, G.D., Goodwin, S., Sutter,**
667 **T.R., Williams, R.W. and Lu, L.** (2006) How replicable are mRNA expression QTL? *Mammalian Genome*,
668 **17**, 643-65610.1007/s00335-005-0187-8.
- 669 **Pincot, D.D.A., Poorten, T.J., Hardigan, M.A., Harshman, J.M., Acharya, C.B., Cole, G.S., Gordon, T.R.,**
670 **Stueven, M., Edger, P.P. and Knapp, S.J.** (2018) Genome-Wide Association Mapping Uncovers
671 *Fw1*, a Dominant Gene Conferring Resistance to Fusarium Wilt in Strawberry. *G3:*
672 *Genes/Genomes/Genetics*, **8**, 181710.1534/g3.118.200129.
- 673 **R. Development Core Team** (2014) R: A language and environment for statistical computing.
- 674 **Rajaraman, J., Douchkov, D., Hensel, G., Stefanato, F.L., Gordon, A., Ereful, N., Caldararu, O.F., Petrescu,**
675 **A.J., Kumlehn, J., Boyd, L.A. and Schweizer, P.** (2016) An LRR/Malectin Receptor-Like Kinase Mediates
676 Resistance to Non-adapted and Adapted Powdery Mildew Fungi in Barley and Wheat. *Front Plant Sci*,
677 **7**, 710.3389/fpls.2016.01836.
- 678 **Roach, J.A., Verma, S., Peres, N.A., Jamieson, A.R., van de Weg, W.E., Bink, M.C.A.M., Bassil, N.V., Lee, S.**
679 **and Whitaker, V.M.** (2016) FaRXf1: a locus conferring resistance to angular leaf spot caused by
680 *Xanthomonas fragariae* in octoploid strawberry. *Theoretical and Applied Genetics*, **129**, 1191-
681 120110.1007/s00122-016-2695-1.
- 682 **Salinas, N., Verma, S., Peres, N. and Whitaker, V.M.** (2018) FaRCa1: a major subgenome-specific locus conferring
683 resistance to *Colletotrichum acutatum* in strawberry. *Theoretical and Applied Genetics*10.1007/s00122-018-
684 3263-7.

- 685 **Stamatakis, A.** (2014) RAxML version 8: a tool for phylogenetic analysis and post-analysis of large phylogenies.
686 *Bioinformatics*, **30**, 1312-1313. [10.1093/bioinformatics/btu033](https://doi.org/10.1093/bioinformatics/btu033).
- 687 **Suyama, M., Torrents, D. and Bork, P.** (2006) PAL2NAL: robust conversion of protein sequence alignments into
688 the corresponding codon alignments. *Nucleic acids research*, **34**, W609-W612
- 689 **Sánchez-Sevilla, J.F., Vallarino, J.G., Osorio, S., Bombarely, A., Posé, D., Merchante, C., Botella, M.A., Amaya,
690 I. and Valpuesta, V.** (2017) Gene expression atlas of fruit ripening and transcriptome assembly from RNA-
691 seq data in octoploid strawberry (*Fragaria × ananassa*). *Scientific Reports*, **7**, 1373710. [10.1038/s41598-017-14239-6](https://doi.org/10.1038/s41598-017-14239-6).
- 693 **Tang, Y., Liu, X., Wang, J., Li, M., Wang, Q., Tian, F., Su, Z., Pan, Y., Liu, D., Lipka, A.E., Buckler, E.S. and
694 Zhang, Z.** (2016) GAPIT Version 2: An Enhanced Integrated Tool for Genomic Association and Prediction.
695 *The Plant Genome*, **9**. [3835/plantgenome2015.11.0120](https://doi.org/10.3835/plantgenome2015.11.0120).
- 696 **Tennessen, J.A., Govindarajulu, R., Ashman, T.-L. and Liston, A.** (2014) Evolutionary Origins and Dynamics of
697 Octoploid Strawberry Subgenomes Revealed by Dense Targeted Capture Linkage Maps. *Genome Biology
698 and Evolution*, **6**, 3295-3313. [10.1093/gbe/evu261](https://doi.org/10.1093/gbe/evu261).
- 699 **van Dijk, T., Pagliarani, G., Pikunova, A., Noordijk, Y., Yilmaz-Temel, H., Meulenbroek, B., Visser, R.G.F.
700 and van de Weg, E.** (2014) Genomic rearrangements and signatures of breeding in the allo-octoploid
701 strawberry as revealed through an allele dose based SSR linkage map. *BMC Plant Biology*, **14**,
702 5510.1186/1471-2229-14-55.
- 703 **Van Ghelder, C. and Esmenjaud, D.** (2016) TNL genes in peach: insights into the post-LRR domain. *BMC
704 Genomics*, **17**, 31710.1186/s12864-016-2635-0.
- 705 **Verma, S., Bassil, N.V., van de Weg, E., Harrison, R.J., Monfort, A., Hidalgo, J.M., Amaya, I., Denoyes, B.,
706 Mahoney, L., Davis, T.M., Fan, Z., Knapp, S. and Whitaker, V.M.** (2017) Development and evaluation
707 of the Axiom® IStraw35 384HT array for the allo-octoploid cultivated strawberry *Fragaria × ananassa*:
708 International Society for Horticultural Science (ISHS), Leuven, Belgium, pp. 75-82.
- 709 **Verma, S., Osorio, L.F., Lee, S., Bassil, N.V. and Whitaker, V.M.** (2018) Genome-Assisted Breeding in the
710 Octoploid Strawberry. In *The Genomes of Rosaceous Berries and Their Wild Relatives* (Hytönen, T., Graham,
711 J. and Harrison, R. eds). Cham: Springer International Publishing, pp. 161-184.
- 712 **Vining, K.J., Salinas, N., Tennessen, J.A., Zurn, J.D., Sargent, D.J., Hancock, J. and Bassil, N.V.** (2017)
713 Genotyping-by-sequencing enables linkage mapping in three octoploid cultivated strawberry families. *PeerJ*,
714 **5**, e373110. [10.7717/peerj.3731](https://doi.org/10.7717/peerj.3731).
- 715 **Wen, Z., Yao, L., Wan, R., Li, Z., Liu, C. and Wang, X.** (2015) Ectopic Expression in *Arabidopsis thaliana* of an
716 NB-ARC Encoding Putative Disease Resistance Gene from Wild Chinese *Vitis pseudoreticulata* Enhances
717 Resistance to Phytopathogenic Fungi and Bacteria. *Frontiers in Plant Science*, **6**, 1087
- 718 **Witek, K., Jupe, F., Witek, A.I., Baker, D., Clark, M.D. and Jones, J.D.G.** (2016) Accelerated cloning of a potato
719 late blight-resistance gene using RenSeq and SMRT sequencing. *Nature Biotechnology*, **34**,
720 65610.1038/nbt.3540
721 <https://www.nature.com/articles/nbt.3540#supplementary-information>.
- 722 **Xiao, S., Ellwood, S., Calis, O., Patrick, E., Li, T., Coleman, M. and Turner, J.G.** (2001) Broad-Spectrum Mildew
723 Resistance in *Arabidopsis thaliana* Mediated by RPW8. [10.1126/science.291.5501.118](https://doi.org/10.1126/science.291.5501.118).
- 724 **Xiong, J.-S., Zhu, H.-Y., Bai, Y.-B., Liu, H. and Cheng, Z.-M.** (2018) RNA sequencing-based transcriptome
725 analysis of mature strawberry fruit infected by necrotrophic fungal pathogen *Botrytis cinerea*. *Physiological
726 and Molecular Plant Pathology*, **104**, 77-85. <https://doi.org/10.1016/j.pmpp.2018.08.005>.
- 727 **Yang, Z.** (2007) PAML 4: phylogenetic analysis by maximum likelihood. *Molecular biology and evolution*, **24**, 1586-
728 1591
- 729 **Zhong, Y. and Cheng, Z.-M.M.** (2016) A unique RPW8-encoding class of genes that originated in early land plants
730 and evolved through domain fission, fusion, and duplication. *Scientific Reports*, **6**,
731 32923. [doi:10.1038/srep32923](https://doi.org/10.1038/srep32923).
- 732 **Zhong, Y., Zhang, X. and Cheng, Z.-M.** (2018) Lineage-specific duplications of NBS-LRR genes occurring before
733 the divergence of six *Fragaria* species. *BMC Genomics*, **19**, 12810.1186/s12864-018-4521-4.

734

735

736

737

Table 1 NLR-gene subtype distribution across three strawberry species

| | <i>cv. Camarosa</i> | <i>F. vesca</i> | <i>F. iinumae</i> |
|---------------------|---------------------|-----------------|-------------------|
| NB | 19.8% | 17.7% | 11.6% |
| NB-LRR | 2.3% | 1.9% | 5.2% |
| NB-only type | 22.1% | 19.6% | 16.8% |
| CC-NB | 16.7% | 12.3% | 32.6% |
| CC-NB-LRR | 3.0% | 2.5% | 2.1% |
| CNL-type | 19.7% | 14.7% | 34.6% |
| RPW | 9.3% | 10.9% | 5.9% |
| RPW-NB | 4.6% | 8.4% | 3.4% |
| RPW-type | 13.9% | 19.3% | 9.3% |
| TIR | 13.7% | 37.1% | 22.2% |
| TIR-NB | 20.0% | 4.9% | 13.2% |
| TIR-NB-LRR | 10.6% | 4.4% | 3.9% |
| TNL-type | 44.3% | 46.3% | 39.3% |

Relative content of NLR-gene subtypes and truncated subtypes are shown.

738

Table 2 Cis Expression-QTL for Strawberry Fruit

| R-gene Name | eQTL phase | IStraw35 AX- | MAF | p-value (FDR) | h ² estimate | Mara | Elyana | Radiance | Festival | Winter dawn | Description |
|--|------------|--------------|------|---------------|-------------------------|------|--------|----------|----------|-------------|---|
| augustus_masked-fvb1-2-processed-gene-27.2 | cis | 89817565 | 0.43 | 0.0418 | 30.4% | 36.6 | 113.3 | 32.2 | 21.3 | 34.3 | uncharacterized protein LOC101293711 |
| augustus_masked-fvb1-4-processed-gene-7.11 | cis | 166502627 | 0.16 | 0.0150 | 43.4% | 2.3 | 0.6 | 4.0 | 3.8 | 1.6 | PLT5_ARATH Sugar-proton symporter PLT5 |
| augustus_masked-fvb2-4-processed-gene-105.5 | cis | 166503861 | 0.29 | 0.0114 | 80.9% | 0.0 | 0.0 | 2.8 | 1.8 | 1.3 | TMVRN_NICGU TMV resistance N |
| augustus_masked-fvb3-1-processed-gene-107.3 | cis | 166511589 | 0.50 | 0.0294 | 41.8% | 0.0 | 0.5 | 0.7 | 0.8 | 0.3 | DRL30_ARATH Probable disease resistance At5g04720 |
| augustus_masked-fvb3-3-processed-gene-283.7 | cis | 89786873 | 0.38 | 0.0009 | 30.4% | 0.8 | 0.4 | 0.0 | 2.6 | 0.4 | DRL1_ARATH Probable disease resistance At1g12280 |
| augustus_masked-fvb3-3-processed-gene-38.8 | cis | 166513199 | 0.23 | 0.0032 | 81.7% | 6.0 | 3.0 | 5.5 | 0.8 | 4.9 | Y4294_ARATH LRR receptor-like serine threonine- kinase |
| augustus_masked-fvb3-4-processed-gene-19.4 | cis | 166504873 | 0.28 | 0.0014 | 100% | 0.1 | 4.8 | 5.6 | 8.0 | 0.1 | DR100_ARATH DNA damage-repair toleration DRT100 |
| augustus_masked-fvb4-1-processed-gene-166.2 | cis | 166505902 | 0.43 | 0.0083 | 91.5% | 0.6 | 0.4 | 2.5 | 1.4 | 1.8 | MKKA_DICDI Mitogen-activated kinase kinase |
| augustus_masked-fvb4-2-processed-gene-107.10 | cis | 166527457 | 0.18 | 0.0202 | 100% | 0.0 | 0.0 | 1.2 | 1.0 | 0.1 | RGA1_SOLBU disease resistance RGA1 RGA3-blb |
| augustus_masked-fvb4-2-processed-gene-258.8 | cis | 166505336 | 0.35 | 0.0015 | 25.1% | 4.6 | 0.0 | 1.4 | 1.3 | 0.1 | LRX2_ARATH Leucine-rich repeat extensin 2 |
| augustus_masked-fvb5-1-processed-gene-238.7 | cis | 123365994 | 0.09 | 0.0012 | 74.1% | 0.8 | 0.8 | 1.4 | 2.8 | 0.5 | HSL1_ARATH Receptor kinase HSL1 HAESA-LIKE1 |
| augustus_masked-fvb5-1-processed-gene-71.8 | cis | 166524323 | 0.48 | 0.0080 | 35.5% | 1.7 | 0.0 | 10.3 | 4.4 | 3.0 | TIR_ARATH Toll interleukin-1 receptor |
| augustus_masked-fvb5-3-processed-gene-135.4 | cis | 166523635 | 0.26 | 0.0124 | 63.7% | 0.5 | 0.2 | 0.1 | 0.0 | 0.0 | MKKA_DICDI Mitogen-activated kinase kinase |
| augustus_masked-fvb5-4-processed-gene-18.1 | cis | 166518037 | 0.35 | 0.0110 | 26.6% | 0.8 | 1.4 | 0.7 | 2.5 | 0.8 | RGA1_SOLBU disease resistance RGA1 RGA3-blb |
| augustus_masked-fvb5-4-processed-gene-241.6 | cis | 123525092 | 0.44 | 0.0007 | 64.9% | 1.4 | 0.1 | 2.5 | 2.1 | 1.8 | LRX2_ARATH Leucine-rich repeat extensin 2 2 LRR |
| augustus_masked-fvb6-1-processed-gene-345.10 | cis | 166524541 | 0.21 | 0.0050 | 31.7% | 1.8 | 0.7 | 4.1 | 4.1 | 2.2 | HSL1_ARATH Receptor kinase HSL1 HAESA-LIKE1 |
| augustus_masked-fvb7-1-processed-gene-57.2 | cis | 166509572 | 0.12 | 0.0003 | 73.3% | 0.5 | 0.2 | 0.6 | 0.2 | 13.2 | TIR_ARATH Toll interleukin-1 receptor |
| augustus_masked-fvb7-2-processed-gene-302.13 | cis | 166517211 | 0.29 | 0.0083 | 69.2% | 2.3 | 0.0 | 2.1 | 0.1 | 0.0 | MKKA_DICDI Mitogen-activated kinase kinase |
| augustus_masked-fvb7-2-processed-gene-53.6 | cis | 166509530 | 0.49 | 0.0118 | 35.7% | 1.2 | 0.2 | 0.5 | 0.4 | 2.2 | RGA1_SOLBU disease resistance RGA1 RGA3-blb |
| augustus_masked-fvb7-2-processed-gene-54.1 | cis | 166509530 | 0.49 | 0.0121 | 100% | 9.9 | 0.1 | 0.4 | 0.3 | 11.5 | LRX2_ARATH Leucine-rich repeat extensin 2 2 LRR |
| maker-fvb1-4-augustus-gene-30.48 | cis | 123365069 | 0.33 | 0.0175 | 63.8% | 2.5 | 0.4 | 3.1 | 4.2 | 2.5 | HSL1_ARATH Receptor kinase HSL1 HAESA-LIKE1 |
| maker-fvb2-1-augustus-gene-182.42 | cis | 89877559 | 0.46 | 0.0225 | 80.9% | 2.1 | 3.8 | 2.2 | 3.2 | 0.8 | MKKA_DICDI Mitogen-activated kinase |
| maker-fvb2-1-snap-gene-111.27 | cis | 166503168 | 0.29 | 0.0002 | 100% | 0.5 | 0.0 | 0.0 | 2.0 | 1.2 | RGA1_SOLBU disease resistance RGA1 RGA3-blb |
| maker-fvb7-1-snap-gene-223.45 | cis | 123540423 | 0.45 | 0.0077 | 70.3% | 2.4 | 0.1 | 0.1 | 0.0 | 1.7 | LRX2_ARATH Leucine-rich repeat extensin 2 2 LRR |
| maker-fvb7-4-snap-gene-48.49 | cis | 166508582 | 0.34 | 0.0357 | 75.1% | 0.3 | 0.4 | 0.1 | 0.0 | 0.2 | HSL1_ARATH Receptor kinase HSL1 HAESA-LIKE1 |
| maker-fvb7-4-snap-gene-59.59 | cis | 166518351 | 0.50 | 0.0064 | 4.7% | 0.9 | 0.4 | 1.8 | 0.1 | 1.6 | TIR_ARATH Toll interleukin-1 receptor |
| maker-fvb7-4-snap-gene-59.63 | cis | 166518351 | 0.50 | 0.0092 | 44.8% | 0.1 | 0.0 | 0.6 | 0.0 | 0.4 | MKKA_DICDI Mitogen-activated kinase |
| maker-fvb7-4-snap-gene-69.51 | cis | 123359450 | 0.17 | 0.0002 | 82.6% | 2.3 | 1.8 | 2.1 | 3.6 | 2.2 | RGA1_SOLBU disease resistance RGA1 RGA3-blb |
| snap_masked-fvb1-2-processed-gene-79.33 | cis | 123359751 | 0.08 | 0.0068 | 98.3% | 0.0 | 0.0 | 0.0 | 0.0 | 2.0 | LRX2_ARATH Leucine-rich repeat extensin 2 2 LRR |
| snap_masked-fvb2-1-processed-gene-107.14 | cis | 89780995 | 0.22 | 0.0011 | 75.1% | 2.1 | 2.6 | 8.5 | 4.0 | 3.4 | HSL1_ARATH Receptor kinase HSL1 HAESA-LIKE1 |
| snap_masked-fvb3-2-processed-gene-11.25 | cis | 166509770 | 0.37 | 0.0084 | 11.4% | 0.2 | 0.2 | 1.1 | 1.5 | 0.7 | TIR_ARATH Toll interleukin-1 receptor |
| snap_masked-fvb3-3-processed-gene-288.15 | cis | 123361033 | 0.45 | 0.0095 | 98.9% | 0.9 | 0.5 | 2.0 | 1.4 | 1.3 | MKKA_DICDI Mitogen-activated kinase kinase A |
| snap_masked-fvb6-1-processed-gene-37.31 | cis | 166519417 | 0.34 | 0.0411 | 24.2% | 13.3 | 19.2 | 0.9 | 0.5 | 0.0 | RGA1_SOLBU disease resistance RGA1 |
| snap_masked-fvb7-2-processed-gene-254.35 | cis | 123357141 | 0.33 | 0.0011 | 36.5% | 0.0 | 0.0 | 0.0 | 0.0 | 0.0 | LRX2_ARATH Leucine-rich repeat extensin 2 2 |
| maker-fvb7-1-snap-gene-273.51 | cis | 166508667 | 0.43 | 0.0319 | 35.7% | 0.0 | 0.0 | 0.0 | 0.4 | 0.0 | Y3475_ARATH LRR receptor-like serine threonine- kinase |
| maker-fvb3-4-augustus-gene-265.40 | cis | 166513103 | 0.13 | 0.0007 | 54.7% | 4.4 | 5.3 | 2.6 | 18.8 | 5.2 | GLO5_ARATH Peroxisomal(S)-2-hydroxy-acid oxidase GLO5 |
| maker-fvb5-1-snap-gene-191.37 | cis | 166523649 | 0.13 | 0.0000 | 36.5% | 0.0 | 0.0 | 0.0 | 0.0 | 0.1 | RPM1_ARATH Disease resistance RPM1 |
| maker-fvb5-2-augustus-gene-59.20 | cis | 123364094 | 0.46 | 0.0036 | 46.0% | 0.0 | 0.3 | 4.0 | 12.0 | 0.8 | probable LRR receptor-like serine threonine- kinase At5g48740 |
| maker-fvb5-2-augustus-gene-61.13 | cis | 123364094 | 0.46 | 0.0014 | 71.7% | 0.0 | 0.3 | 2.2 | 1.6 | 0.8 | P2B10_ARATH F-box PP2-B10 PHLOEM PROTEIN 2-LIKE |
| maker-fvb5-2-augustus-gene-63.17 | cis | 123364094 | 0.46 | 0.0072 | 16.5% | 0.0 | 0.0 | 3.5 | 3.7 | 1.1 | P2B11_ARATH F-box PP2-B11 PHLOEM PROTEIN 2-LIKE |
| maker-fvb5-2-snap-gene-4.75 | cis | 166506813 | 0.32 | 0.0000 | 29.9% | 2.1 | 9.3 | 37.2 | 43.0 | 1.4 | DRL28_ARATH Probable disease resistance At4g27220 |
| maker-fvb5-2-snap-gene-61.17 | cis | 123364094 | 0.46 | 0.0291 | 78.4% | 0.0 | 0.2 | 1.3 | 1.4 | 0.3 | P2B11_ARATH F-box PP2-B11 PHLOEM PROTEIN 2-LIKE |
| maker-fvb5-3-augustus-gene-135.25 | cis | 89832439 | 0.37 | 0.0040 | 11.5% | 0.0 | 0.0 | 1.6 | 0.3 | 1.3 | RPM1_ARATH Disease resistance RPM1 |
| maker-fvb4-3-snap-gene-155.68 | cis | 123524810 | 0.21 | 0.0016 | 100% | 0.1 | 0.2 | 0.6 | 0.1 | 0.5 | TMVRN_NICGU TMV resistance N |
| maker-fvb5-3-snap-gene-221.67 | cis | 89893608 | 0.11 | 0.0045 | 94.4% | 0.5 | 0.2 | 0.1 | 1.6 | 0.1 | TMVRN_NICGU TMV resistance N |
| maker-fvb5-3-snap-gene-254.50 | cis | 166523796 | 0.21 | 0.0155 | 51.8% | 0.1 | 0.1 | 6.4 | 0.5 | 0.1 | TMVRN_NICGU TMV resistance N |
| maker-fvb5-4-snap-gene-125.42 | cis | 166506186 | 0.18 | 0.0078 | 93.2% | 0.6 | 0.0 | 2.0 | 2.3 | 1.4 | RGA3_SOLBU RGA3 Blight resistance B149 |
| maker-fvb6-1-augustus-gene-153.32 | cis | 166507404 | 0.17 | 0.0000 | 76.3% | 0.0 | 0.0 | 23.5 | 6.8 | 17.5 | RGA3_SOLBU RGA3 Blight resistance B149 |
| maker-fvb5-2-augustus-gene-61.14 | cis | 123364473 | 0.47 | 0.0167 | 44.9% | 0.0 | 0.1 | 0.7 | 1.2 | 0.3 | P2B10_ARATH F-box PP2-B10 PHLOEM PROTEIN 2-LIKE |
| augustus_masked-fvb7-1-processed-gene-284.2 | cis | 123359573 | 0.4 | 0.0139 | 95.1% | 0.3 | 0 | 0.1 | 0.3 | 0.2 | EMS1_ARATH Leucine-rich repeat receptor kinase EMS1 |
| snap_masked-fvb6-2-processed-gene-263.31 | cis | 89781514 | 0.24 | 0.0084 | 54.9% | 0 | 0 | 4.3 | 4.3 | 2.2 | TMVRN_NICGU TMV resistance N |
| maker-fvb7-2-snap-gene-161.50 | cis | 123364494 | 0.39 | 0.0052 | 38.9% | 2.4 | 1 | 4 | 2 | 2.6 | MAP1A_ARATH Methionine aminopeptidase 1A MAP 1A 1A |
| maker-fvb6-1-augustus-gene-160.45 | cis | 166515747 | 0.21 | 0.0340 | 38.4% | 12.6 | 8.8 | 11.9 | 4.2 | 10.3 | DGK5_ARATH Diacylglycerol kinase 5 |

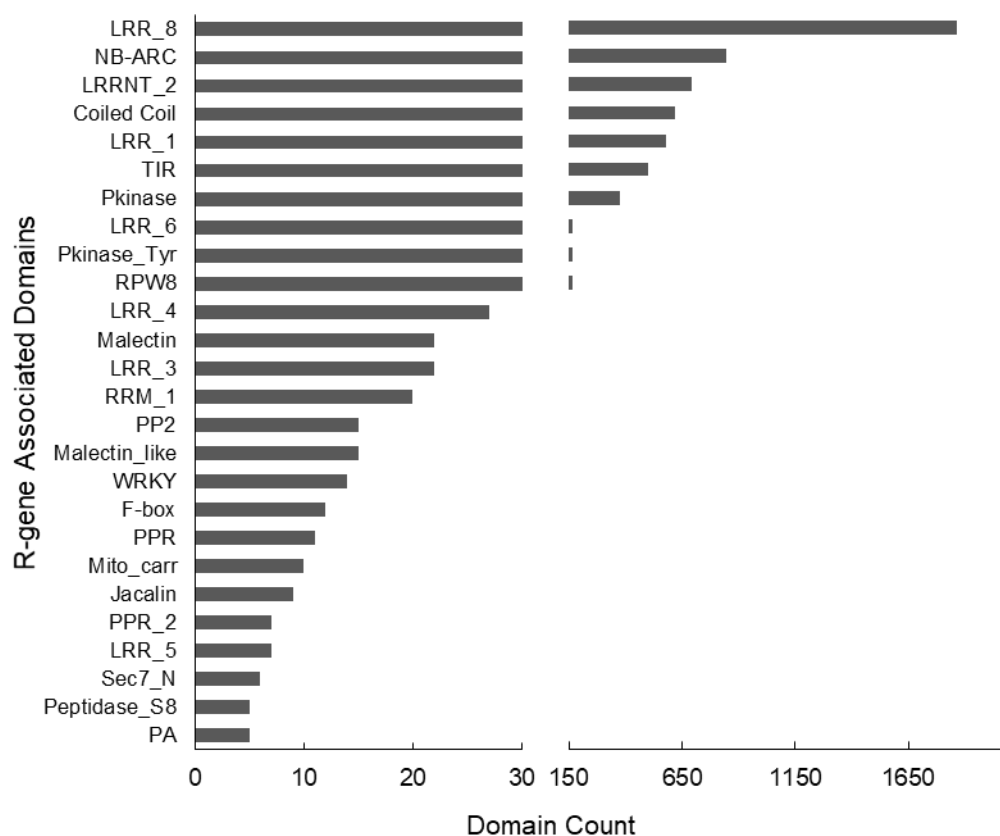
Genetic association results for 61 transcriptomes are shown, detailing cis genetic factors controlling differentially expressed R-genes. The most significant marker name, minor allele frequency, FDR-adjusted p-value, narrow sense heritability, transcript accumulation in cultivars, and BLAST2GO description are shown.

Table 3 Trans and Cis Expression-QTL for Strawberry Fruit

| R-gene Name | eQTL phase | IStraw35 AX- | MAF | p-value (FDR) | h ² estimate | Mara | Elyana | Radiance | Festival | Winter dawn | Description |
|--|------------|--------------|------|---------------|-------------------------|------|--------|----------|----------|-------------|--|
| maker-fvb4-2-snap-gene-5.61 | cis | 166505436 | 0.38 | 0.0214 | 34.3% | 1.5 | 0.9 | 1.6 | 3.0 | 2.3 | PSKR1_ARATH LRR receptor kinase 1 serine-threonine |
| | trans | 123361503 | 0.38 | 0.0214 | | | | | | | |
| maker-fvb5-1-augustus-gene-139.47 | cis | 123524951 | 0.28 | 0.0482 | 77.5% | 0.3 | 0.4 | 5.8 | 1.5 | 1.0 | PIRL5_ORYSJ Plant intracellular Ras-group-related LRR 5 |
| | trans | 123361742 | 0.14 | 0.0482 | | | | | | | |
| maker-fvb5-1-augustus-gene-263.34 | cis | 123357041 | 0.18 | 0.0415 | 14.6% | 8.6 | 4.0 | 3.3 | 3.7 | 3.2 | R13L1_ARATH disease resistance RPP13 1 |
| | trans | 166506561 | 0.18 | 0.0415 | | | | | | | |
| maker-fvb5-2-snap-gene-213.46 | cis | 89817904 | 0.10 | 0.0006 | 79.8% | 1.7 | 1.6 | 3.3 | 0.0 | 1.4 | DRL21_ARATH disease resistance At3g14460 |
| | trans | 123539826 | 0.10 | 0.0006 | | | | | | | |
| maker-fvb5-2-snap-gene-46.64 | cis | 166506808 | 0.48 | 0.0192 | 67.1% | 3.4 | 0.0 | 1.3 | 1.0 | 1.4 | GSO1_ARATH LRR receptor-like serine threonine- kinase |
| | trans | 166522785 | 0.48 | 0.0192 | | | | | | | |
| maker-fvb5-3-snap-gene-244.48 | cis | 123367068 | 0.48 | 0.0046 | 39.5% | 0.4 | 0.5 | 4.7 | 5.6 | 2.8 | Y4265_ARATH Probable LRR receptor-like serine threonine- |
| | trans | 166524268 | 0.48 | 0.0046 | | | | | | | |
| maker-fvb5-4-snap-gene-110.38 | cis | 166523511 | 0.21 | 0.0001 | 100% | 1.0 | 1.3 | 0.4 | 1.6 | 0.3 | PIRL5_ORYSJ Plant intracellular Ras-group-related LRR 5 |
| | trans | 166524147 | 0.29 | 0.0014 | | | | | | | |
| maker-fvb6-1-augustus-gene-27.58 | cis | 123363787 | 0.38 | 0.0028 | 91.2% | 0.3 | 0.0 | 0.2 | 0.5 | 0.0 | DRL42_ARATH Probable disease resistance At5g66900 |
| | trans | 123358884 | 0.38 | 0.0028 | | | | | | | |
| maker-fvb6-3-snap-gene-412.71 | cis | 123614270 | 0.27 | 0.0457 | 74.4% | 1.8 | 1.1 | 1.4 | 2.1 | 0.9 | TIR_ARATH Toll interleukin-1 receptor |
| | trans | 166525307 | 0.27 | 0.0457 | | | | | | | |
| augustus_masked-fvb6-2-processed-gene-268.10 | cis | 166525890 | 0.48 | 0.0021 | 91.2% | 0.8 | 0.8 | 0.3 | 1.7 | 1.2 | HSL1_ARATH Receptor kinase HSL1 HAESA-LIKE1 |
| | trans | 123362183 | 0.48 | 0.0021 | | | | | | | |
| augustus_masked-fvb6-3-processed-gene-176.9 | cis | 166515622 | 0.33 | 0.0004 | 65.6% | 0.4 | 0.0 | 7.9 | 20.0 | 0.1 | ADT3_ARATH ADP,ATP carrier mitochondrial ADP ATP |
| | trans | 123525691 | 0.33 | 0.0005 | | | | | | | |
| augustus_masked-fvb7-2-processed-gene-63.0 | cis | 166508452 | 0.30 | 0.0047 | 27.7% | 0.5 | 0.1 | 1.3 | 0.1 | 0.0 | TMVRN_NICGU TMV resistance N |
| | trans | 89823698 | 0.28 | 0.0047 | | | | | | | |
| augustus_masked-fvb7-3-processed-gene-243.6 | cis | 166517344 | 0.38 | 0.0204 | 66.5% | 47.5 | 14.1 | 0.1 | 8.1 | 0.7 | DR100_ARATH DNA damage-repair toleration DRT100 |
| | trans | 89894427 | 0.38 | 0.0204 | | | | | | | |
| maker-fvb1-2-snap-gene-63.40 | cis | 166510935 | 0.17 | 0.0015 | 86.2% | 0.5 | 0.1 | 1.3 | 0.1 | 0.0 | TMVRN_NICGU TMV resistance N |
| | trans | 166525497 | 0.16 | 0.0015 | | | | | | | |
| maker-fvb1-2-snap-gene-96.40 | cis | 166517617 | 0.18 | 0.0020 | 67.6% | 0.0 | 0.0 | 1.0 | 0.0 | 0.4 | DRL42_ARATH Probable disease resistance |
| | trans | 166525528 | 0.18 | 0.0020 | | | | | | | |
| maker-fvb1-4-snap-gene-66.72 | cis | 123363545 | 0.28 | 0.0280 | 68.4% | 3.9 | 0.2 | 12.0 | 12.0 | 7.4 | U496I_ARATH UPF0496 At2g18630 |
| | trans | 166516240 | 0.18 | 0.0093 | | | | | | | |
| maker-fvb1-4-snap-gene-76.45 | cis | 123357162 | 0.18 | 0.0001 | 100% | 0.7 | 0.2 | 0.0 | 0.0 | 0.0 | DRL43_ARATH Probable disease resistance |
| | trans | 166516240 | 0.18 | 0.0001 | | | | | | | |
| maker-fvb7-2-augustus-gene-136.47 | cis | 166526312 | 0.43 | 0.0116 | 79.9% | 0.3 | 0.0 | 0.4 | 0.4 | 0.2 | TMVRN_NICGU TMV resistance N |
| | trans | 123359434 | 0.46 | 0.0371 | | | | | | | |
| maker-fvb7-2-augustus-gene-147.47 | cis | 123359385 | 0.45 | 0.0003 | 45.2% | 1.1 | 0.2 | 5.5 | 3.1 | 2.1 | TMVRN_NICGU TMV resistance N |
| | trans | 123365359 | 0.42 | 0.0011 | | | | | | | |
| maker-fvb7-2-augustus-gene-163.44 | cis | 123364494 | 0.39 | 0.0011 | 52.3% | 0.7 | 0.3 | 2.0 | 0.9 | 0.8 | RGA3_SOLBU disease resistance RGA3 Blight resistance |
| | trans | 123365359 | 0.42 | 0.0055 | | | | | | | |
| maker-fvb7-2-augustus-gene-65.21 | cis | 166512110 | 0.21 | 0.0031 | 69.2% | 5.3 | 0.3 | 0.9 | 1.2 | 0.5 | RP8L2_ARATH Probable disease resistance RPP8 2 |
| | trans | 166509598 | 0.21 | 0.0031 | | | | | | | |
| maker-fvb7-2-snap-gene-161.50 | cis | 123364494 | 0.39 | 0.0052 | 38.9% | 2.4 | 1.0 | 4.0 | 2.0 | 2.6 | MAP1A_ARATH Methionine aminopeptidase 1A MAP 1A 1A |
| | trans | 123365359 | 0.42 | 0.0154 | | | | | | | |
| snap_masked-fvb3-4-processed-gene-8.19 | cis | 166521734 | 0.16 | 0.0023 | 69.6% | 2.2 | 4.3 | 6.2 | 5.2 | 4.0 | TMVRN_NICGU TMV resistance N |
| | trans | 89826525 | 0.17 | 0.0033 | | | | | | | |
| snap_masked-fvb6-1-processed-gene-352.19 | cis | 123366334 | 0.27 | 0.0306 | 76.8% | 0.1 | 0.0 | 0.8 | 1.1 | 0.8 | TMVRN_NICGU TMV resistance N |
| | trans | 123357007 | 0.42 | 0.0465 | | | | | | | |

Genetic association results for 61 transcriptomes are shown, detailing cis genetic factors controlling differentially expressed R-genes. The most significant marker name, minor allele frequency, FDR-adjusted p-value, narrow sense heritability, transcript accumulation in cultivars, and BLAST2GO description are shown.

743

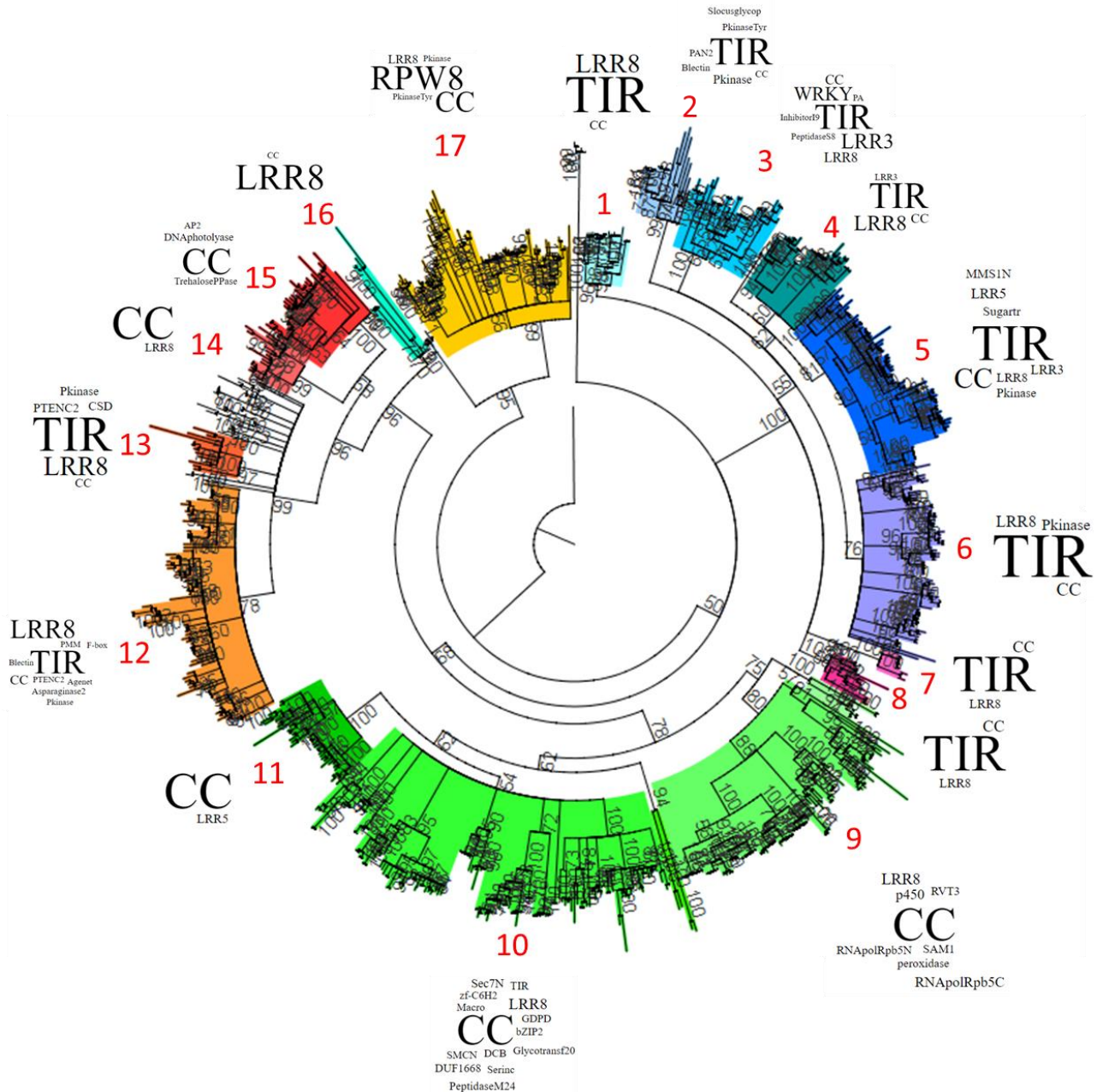


744

745

746 **Figure 1 Canonical and non-Canonical Domains in Strawberry R-Genes.** Classic TNL/CNL-
747 type R-gene domains (TIR, NB-ARC, LRR, etc.) comprise the majority of domain classes in
748 predicted R-genes, however a number of atypical domains are observed in high frequency.
749 Domains below a count of five are not shown.

750

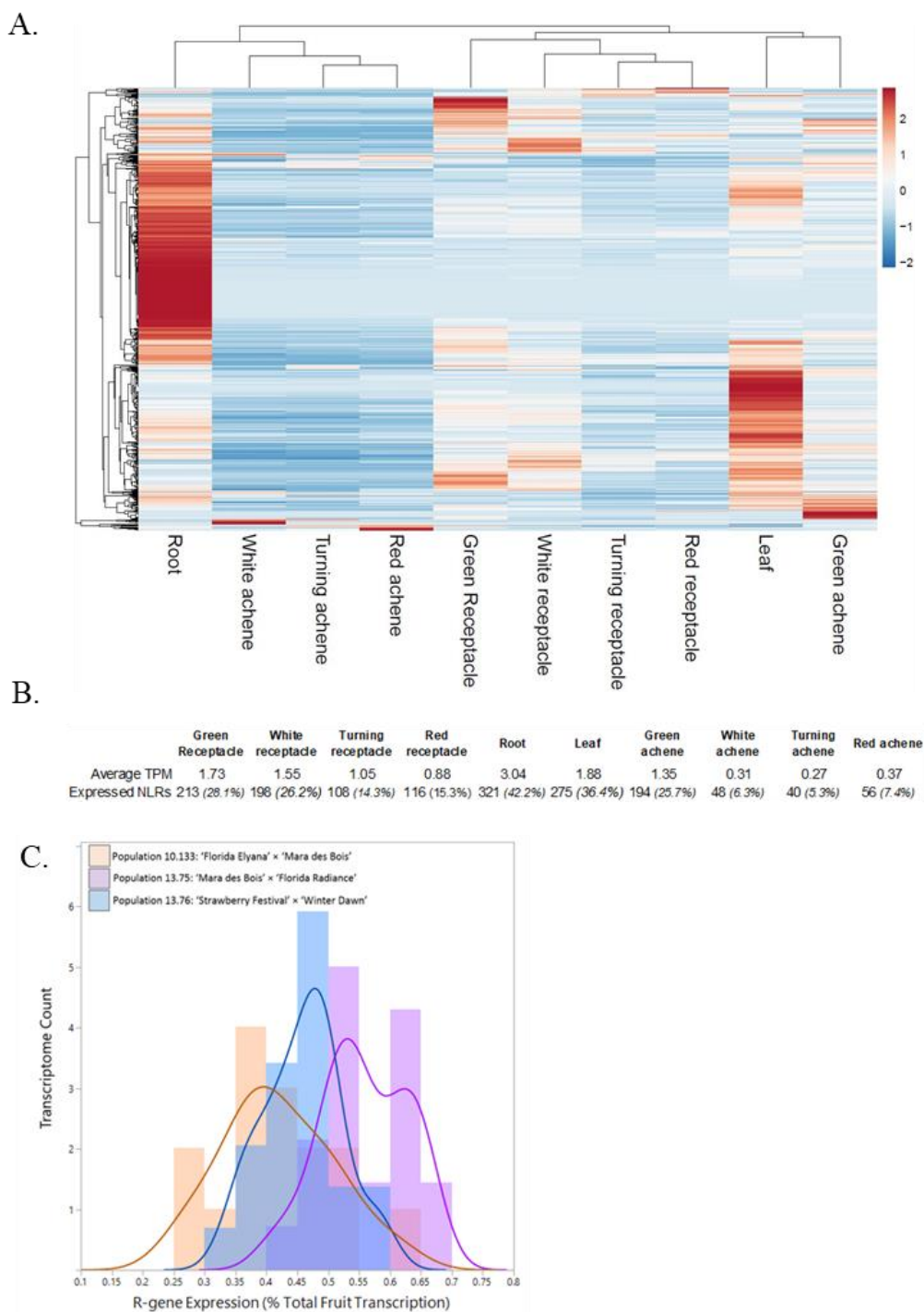


751

752

753 **Figure 2 Phylogenetic Relationship of NB-ARC domains in *F. vesca*, *F. iinumae*, & *F. x***
 754 ***ananassa* ‘Camarosa’.** A. Full-length NB-ARC domains from strawberry *spp.* organize into
 755 clades based on NLR-gene subtype (CC, TIR, NB-ARC, LRR, and RPW-containing
 756 combinations). Maximum likelihood bootstrap values (100 replicates) above a threshold of 50%
 757 are shown with the NB-ARC domain from human *Apaf1* as the outgroup. Word sizes correspond
 758 to relative domain content within each clade.

759

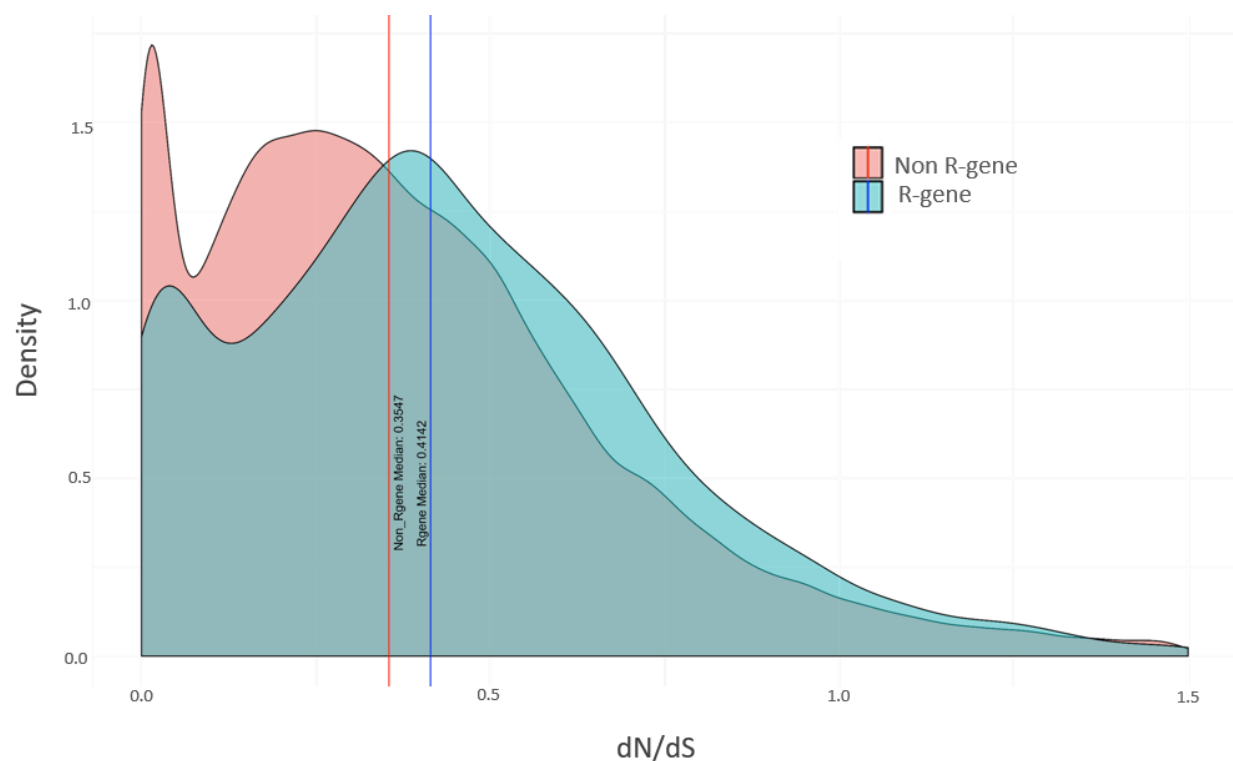


760

761

762 **Figure 3 RNaseq Expression of Octoploid NLR genes.** A. Tissue-based heatmap of scaled
 763 NLR transcript accumulation. B. Averaged NLR transcript abundance (TPM) and total number
 764 of putative expressed NLRs (TPM >1) are reported. The percent of all 756 NLR genes putatively
 765 expressed in each tissue are shown in parentheses. C. Generalized R-gene fruit expression across
 766 three segregating populations (n=61).

767



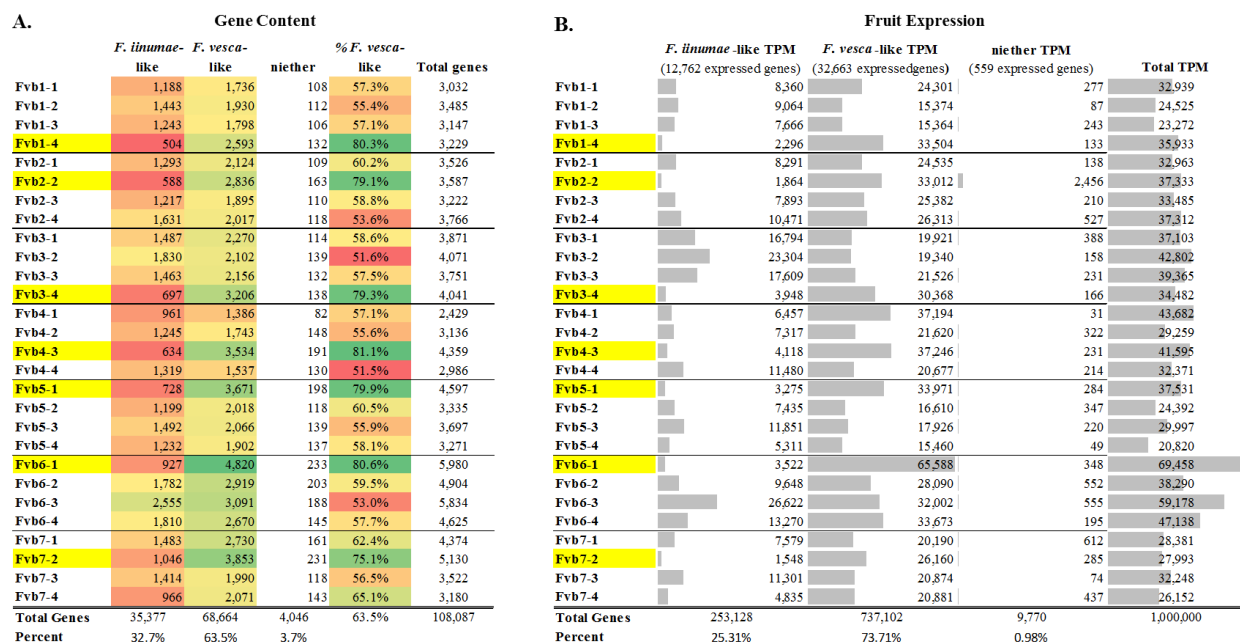
768

769

770 **Figure 4 Evolutionary Pressures on *F. × ananassa* R-genes.** The median dN/dS ratio for R-
771 genes (0.4142) is higher than for non R-genes (0.3547). Density curves for *F. × ananassa* R-genes
772 (blue) and non R-genes (red) are calculated based on comparison to the closest ancestral diploid
773 homolog from *F. vesca*.

774

775

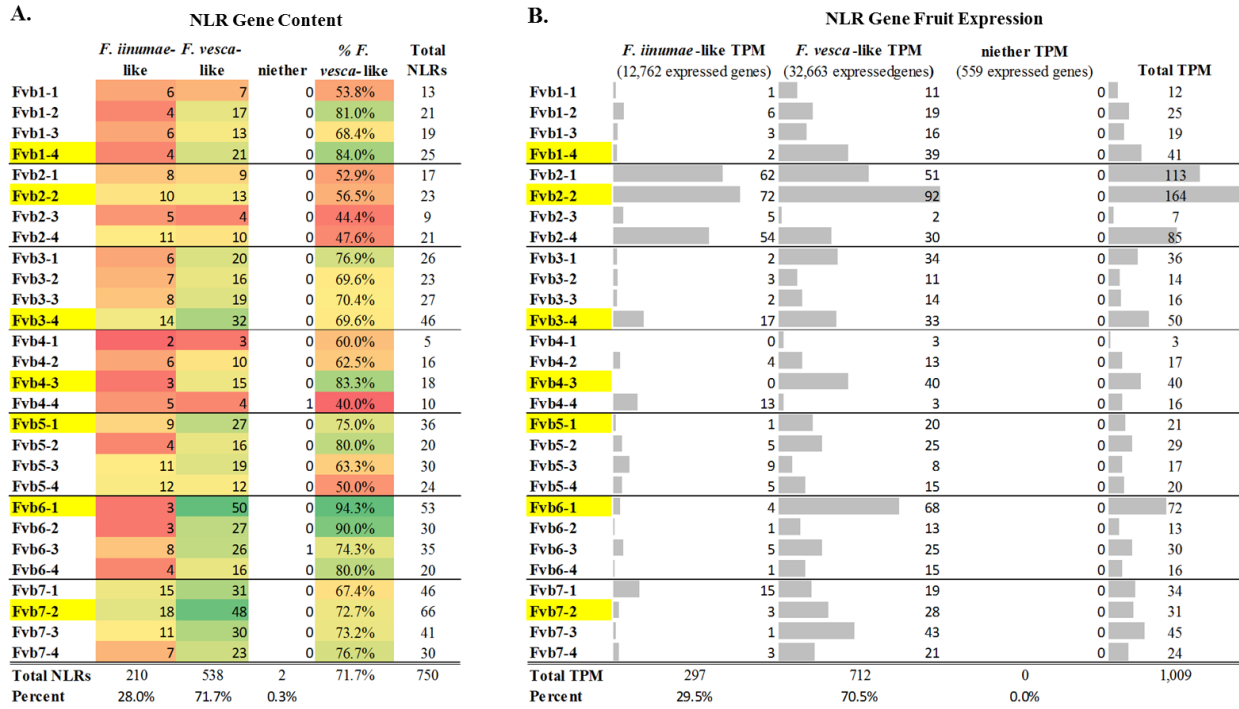


776

777

778 **Figure 5 General Retention and Expression Bias in Octoploid Strawberry.** ‘Camarosa’ gene
 779 models are categorized as either more *F. vesca*-like, more *F. iinumae*-like, or neither. Red-green
 780 color scale indicates low-to-high gene content, respectively. Yellow highlight indicates the most
 781 *F. vesca*-like homoeolog. **A.** Gene content per homeologous chromosome, by putative ancestral
 782 gene similarity. **B.** Relative transcript accumulation of all genes in the fruit, by putative ancestral
 783 similarity.

784



785

786

787

788

789

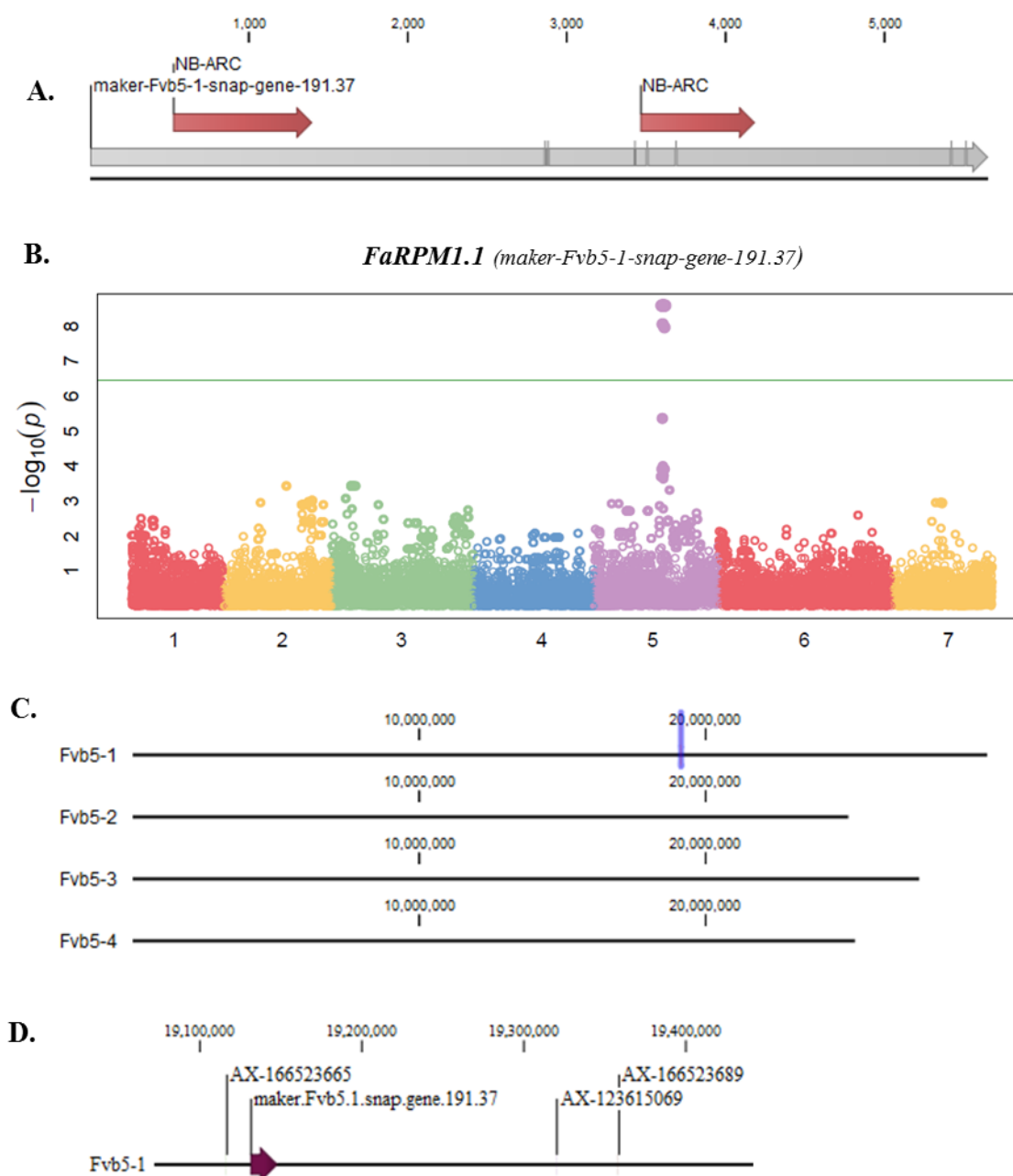
790

791

792

793

Figure 6 NLR-gene Retention and Expression Bias in Octoploid Strawberry. ‘Camarosa’ gene models are categorized as either more *F. vesca*-like, more *F. iinumae*-like, or neither. Red-green color scale indicates low-to-high gene content, respectively. Yellow highlight indicates the most *F. vesca*-like homoeolog. **A.** NLR-gene content per homeologous chromosome, by putative ancestral gene similarity. **B.** Relative transcript accumulation of NLR-genes in the fruit, by putative ancestral similarity.

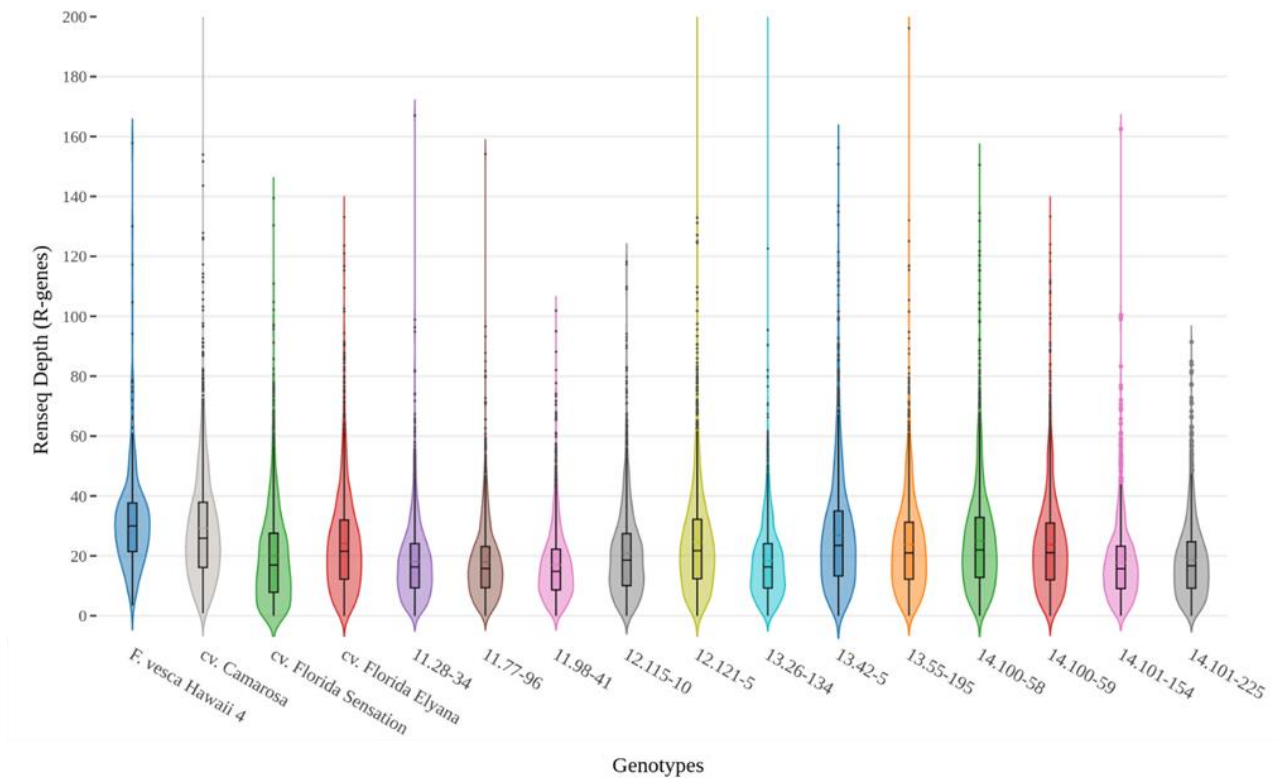


794

795

796 **Figure 7 Example *cis*-eQTL of a Fruit-Expressed Strawberry R-gene.** **A.** Domain analysis of
 797 the ‘Camarosa’ putative resistance gene *FaRPM1.1* indicates two NB-ARC domains. Grey lines
 798 delineate exon-exon borders in the mature predicted transcript. **B.** Octoploid fruit expression of
 799 *FaRPM1.1* associates with a single locus on chromosome 5. **C.** The *Fvb5-1* subgenomic location
 800 of *FaRPM1.1* in the octoploid ‘Camarosa’ genome is indicated (purple vertical line). **D.** Three
 801 equally highly-significant GWAS markers (p -value $8.09E-06$, post-FDR adjustment) show close
 802 subgenome co-localization with *FaRPM1.1*.

803



804

805

806 **Figure 8 RenSeq Increases Sequencing Depth for R-gene Loci in Multiplexed Octoploid**
807 **Genomes.** Sixteen disease-resistant strawberry genomic libraries (fifteen octoploid accessions and
808 diploid *F. vesca*) were enriched for R-genes and sequenced via Illumina Hiseq yielding an average
809 of 2.60 million reads per genomic library. Roughly half of all sequencing reads mapped to a
810 previously-identified R-gene locus, representing a substantial sequence enrichment relative to R-
811 gene genomic representation.

812